Ménard Lecture
The pressuremeter test: Expanding its use

Conférence Ménard
L'essai pressiometrique : élargissement de son utilisation

Briaud J.-L.
President of ISSMGE, Professor, Texas A&M University, Zachry Dpt. of Civil Engineering, College Station, Texas, 77843-3136, USA

ABSTRACT: The purpose of this contribution is to show how the use of the PMT can be expanded further than current practice. The topics covered in a first part include the amount of soil testing necessary to meet a reliability target, the influence of the lack of tensile resistance of soils on the PMT modulus, how to recreate the small strain early part of the curve lost by the decompression-recompression process associated with the preparation of the PMT borehole, best practice for preparing the PMT borehole, commonly expected values of PMT parameters, the use of the PMT unload-reload modulus, and correlations with other soil parameters. The second part deals with foundation engineering and includes the use of the entire expansion curve to predict the load settlement behavior of shallow foundations, the load displacement behavior of deep foundations under horizontal loading, foundation design of very tall structures, long term creep loading, cyclic loading, and dynamic vehicle impact. Finally an attempt is made to generate preliminary soil liquefaction curves base on the normalized PMT limit pressure.

RÉSUMÉ : Le but de cette contribution est de montrer comment l'utilisation du PMT peut être étendu au-delà de la pratique courante. Les sujets abordés dans une première partie comprennent la quantité de reconnaissance de sol nécessaire pour atteindre un objectif de fiabilité, l'influence de l'absence de résistance des sols à la traction sur le module du PMT, comment recréer la partie de la courbe en petites déformations perdue pendant la décompression-recompression associée à la préparation du trou de forage, les meilleures pratiques pour la préparation du trou de forage, les valeurs communes des paramètres PMT, l'utilisation du module décharge-recharge, et des corrélations avec d'autres paramètres du sol. La deuxième partie traite des travaux de fondation et les sujets suivants sont abordés: l'utilisation de la courbe d'expansion du PMT pour prédire le comportement des fondations superficielles, et le comportement des fondations profondes sous charge horizontale, la conception des fondations des structures de grande hauteur, le comportement de fluage, chargement cyclique, et chargement par impact de véhicules. Enfin, on propose des courbes préliminaires de liquéfaction du sol sur la base de la pression limite normalisée du PMT.

KEYWORDS: pressuremeter, modulus, limit pressure, shallow foundations, deep foundations, retaining walls, liquefaction.

1 HOW I GOT INTERESTED IN THE PMT?

The year is 1974 and I am a Master student at the University of New Brunswick, Canada working with Arvid Landva. I had learnt that the triaxial test was the reference test in the laboratory. I had also read from Terzaghi that the action was in the field. So I sat down one late afternoon and tried to invent an in situ triaxial test. I drew some complex systems with double tube samplers and the pressure applied between the two tubes on an internal membrane. It was very complicated and failed the Einstein test of optimum simplicity. I had also learnt from many months behind a drill rig that anything complicated had very little chance of success in the field so I kept searching and designing and then it dawned on me. What if I inverted the problem, drew an inside out triaxial test, and applied the pressure from inside the tube and pushed outward on the soil. And so I designed my first pressuremeter. I was very excited about my new invention and could not sleep that night. I waited anxiously to go to the library the next morning to see what I could dig on this idea. I went to the library and there it was Louis Menard 1957, Jean Kerisel as his advisor, the Master in Illinois with Ralph Peck, the development of the design rules, Sols Soils, 1963 and on and on. I came out of the library that morning, very disappointed that my idea had already been invented. After much reflection that day, I finally decided that I should be happy because it was obviously a good idea since it had received that much attention. This is how I got interested in the pressuremeter. I then went to The University of Ottawa to work with Don Shields who was connected with Francois Baguelin and Jean Francois Jezequel writing the pressuremeter book. Don gave me the manuscript in early Sept 1976 and said read this and correct any mistake. I did and came back 3 months later with the corrected manuscript again rather depressed and telling Don, there is nothing left for me to do, everything has been done. Don smiled and told me don't worry, there is much more to be done on the PMT; I feel that it is still true today and, in fact, it is the topic of this lecture. So this is my story on the PMT and I have been a fan of the PMT ever since.

2 SPECIAL THANKS TO LOUIS MENARD

I met Louis Menard (Fig. 1) on 15 December 1977, one month before he died of cancer. I was a PhD student at the University of Ottawa in Canada working on my pressuremeter research with Don Shields. I was coming back home for Christmas that year and Louis Menard was kind enough to take some time from his very busy schedule to visit with me at the Techniques Louis Menard in Longjumeau near Paris. I waited for 30 minutes but finally got to meet the man who had invented the tool I was so fond of. Around 7 o'clock that day, I entered a huge deep office much like you see in castles. At the other end behind a big desk was Louis Menard waving at me to come closer and take a seat. I introduced myself and we started to talk about the pressuremeter. Very quickly, I found myself enjoying the discussion and time flew by. We talked and argued and talked again and quoted data and theory and reasoning so much so that at the end we had connected. I was mad because I promised myself that I would take notes of what Menard was saying but in the heat of the action I forgot all about it and was left with no notes and it was already 8 O'clock. This is where I got really lucky. Louis Menard asked me: "do you have any plans tonight? I said no and he said: "why don't you stay for dinner?" Whaoh! That would be wonderful. We got up and he took his cane to walk from his office to his house which was a

door away. The cancer was very advanced but he explained to me as we walked to the dining room that he had a slight illness but that he would take care of that in no time! This is where I got my first clue of the remarkable strength of his will power, the steely determination of Louis Menard, a trait of character which helped him win against all odds while creating some slight antagonistic situations. The dinner was a delight. Honestly, I cannot tell you what I ate but I certainly remember the stories that he told me with his wife and his children around the table. One stands out in my mind: his first encounter with Ralph Peck. He said that he entered Professor Peck's office and Peck proceeded to explain to young Louis Menard that he would have to take a certain number of core courses to get his Master degree. So Peck walked to the small blackboard in his office and wrote a list of these 4 or 5 courses, then went back to his desk. Louis Menard got up, took the eraser and wiped the courses out and said I am not interested in these courses; however I am interested in these courses instead. Menard was indeed a very bright, very determined independent thinker. On that day of 15 December 1977 he provided me with a wonderful moment in my life, one that I will never forget.

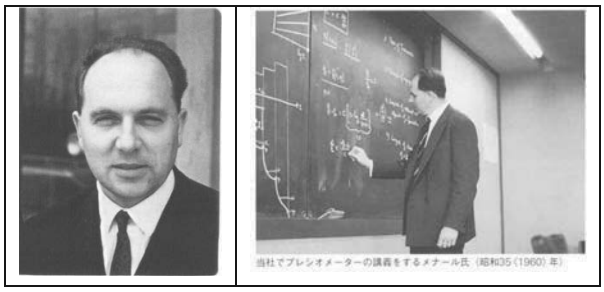

Figure 1. Louis Menard *(courtesy of Michel Gambin and Kenji Mori)*

3 INTRODUCTION

There are many different types of pressuremeter devices and many ways to insert the pressuremeter probe in to the ground. This paper is limited to the preboring pressuremeter also called Menard pressuremeter where a borehole is drilled, the drilling tool is removed, and the probe is lowered in the open hole. The probe diameter is in the range of 50 to 75 mm and the length of the inflatable part of the probe in the range of 0.3 to 0.6 m. The paper starts with a general observation regarding site investigations, then deals with many aspects of the pressuremeter practice including the device itself, the installation, the test, the parameters that can be obtained, and their use in foundation engineering. In each topic, new contributions are made to expand the use of the PMT.

4 HOW MANY BORINGS ARE ENOUGH?

What percentage of the total soil volume involved in the soil response should be tested during the geotechnical investigation. This depends on many factors including the goal of the investigation. This goal may be that there is a high probability that the predictions will be within a target tolerance. As an example of calculations, assume that the block of soil which will be loaded by the structure is a cube 10 x 10 x 10 m in size. Further assume that the goal is to predict the elastic settlement of the structure with a precision of + or – 20% and that the soil cube has a modulus with a coefficient of variation equal to 0.3. The question is: what percentage of the total volume of soil must be tested to have a 98% probability that the predicted settlement will be within + or - 20% of the true settlement (i.e.: measured)? Since in this case the modulus is linearly proportional to the settlement, the question can be rephrased to read: what percentage of the soil volume must be tested so that the mean modulus measured on the soil samples has a 98% confidence level of being within + or – 20% of the true mean of the modulus?

For this we recall the student t distribution. Consider a large population (the big cube) of modulus E which is normally distributed with a mean μ_p and a standard deviation σ_p. Then consider a group of n randomly selected values of the modulus (E_1, E_2, E_3, …, E_n) from the population (results of the site investigation and testing). The mean modulus value of the group E_1, …, E_n, is μ_g and the standard deviation is σ_g. Let's create many such groups of n modulus values (many options of where to drill and where to test), each time randomly selecting n values from the larger population of modulus and calculating the mean modulus μ_g of the group. In this fashion we can create a distribution of the means μ_g. It can be shown that the distribution of the means μ_g has a mean $\mu_{\mu g}$ equal to μ_p and a standard deviation $\sigma_{\mu g}$ equal to $\sigma_p/n^{0.5}$. If we form the normalized variable t:

$$t = \frac{\mu_g - \mu_p}{\sigma_g / \sqrt{n}} \tag{1}$$

then the distribution of t is the student t distribution for n degrees of freedom: t(n). The t distribution is more scattered than the normal distribution of E, depends on the number n of modulus values collected in each group, and tends towards the normal distribution when n becomes large (Fig. 2).

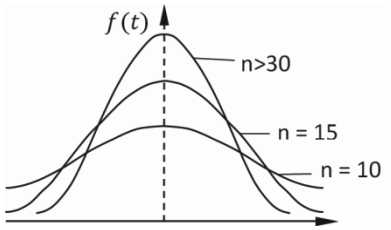

Figure 2. The student t distribution

The properties of the student t distribution together with Eq.1 allow us to write:

$$P\left(\left(\mu_g - t_{\frac{\alpha}{2},n-1}\frac{\sigma_g}{\sqrt{n}}\right) < \mu_p < \left(\mu_g + t_{\frac{\alpha}{2},n-1}\frac{\sigma_g}{\sqrt{n}}\right)\right) = 1-\alpha \tag{2}$$

Where t(α/2,n-1) is the value of t for n-1 degrees off freedom and a value of α/2, α is the area under the t distribution for values larger than t (Fig. 3). Eq.2 expresses that there is a (1-α) degree of confidence that the value of μ_p is between the values expressed in the parenthesis.

For our example, we need to determine the number n of modulus values in the group (number of samples to be collected and tested during the site investigation) which will lead to a high probability P that the predicted modulus (μ_g) will be within a target tolerance Δ from the true mean modulus of the population (μ_p). Therefore we wish to find the value of n which will satisfy the probability equation:

$$P\left(\mu_g(1-\Delta) < \mu_p < \mu_g(1+\Delta)\right) = P_{\text{target}} \tag{3}$$

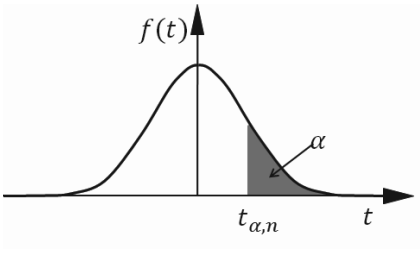

Figure 3. Definition of the parameter α.

That is to say we have a P_{target} % degree of confidence that μ_p lies in the range $\mu_g(1+\text{or}-\Delta)$. We can rewrite Eq.3 as

$$P\left(-\Delta < \frac{\mu_p - \mu_g}{\mu_g} < +\Delta\right) = P_{\text{target}} \quad (4)$$

If the coefficient of variation of the population is δ, then we assume that the coefficient of variation of the group is also δ.

$$\delta = \frac{\sigma_p}{\mu_p} \approx \frac{\sigma_g}{\mu_g} \quad (5)$$

Combining Eq.2, 4, and 5 we get.

$$\mu_g \Delta = t_{\frac{\alpha}{2},n-1} \frac{\sigma_g}{\sqrt{n}} \quad or \quad n = \left(\frac{\delta}{\Delta}\right)^2 \left(t_{\frac{\alpha}{2},n-1}\right)^2 \quad (6)$$

Eq. 6 is solved by iteration since n influences the value of t. Student t distribution solvers are available on the internet. The number n represents the number of soil samples to be tested in order to obtain the value of the modulus within plus or minus Δ% from the exact answer with a P_{target} probability of success. If we assume that a triaxial test sample to obtain a modulus value has a volume of 10^{-3} m^3, then the number n of samples gives the volume of soil that must be drilled during the investigation to satisfy the criterion. The percent volume tested becomes

$$\frac{V_s}{V_t} = \frac{n \times 10^{-3}}{V_t} \quad (7)$$

In our example the initial volume was 1000 m^3, so we can calculate what percentage of the soil volume should be tested. Fig. 4 gives the results and indicates that in order to be 98% sure that the answer will be within plus or minus 20% from the true value, the amount of sampling is 0.001 percent of the total volume.

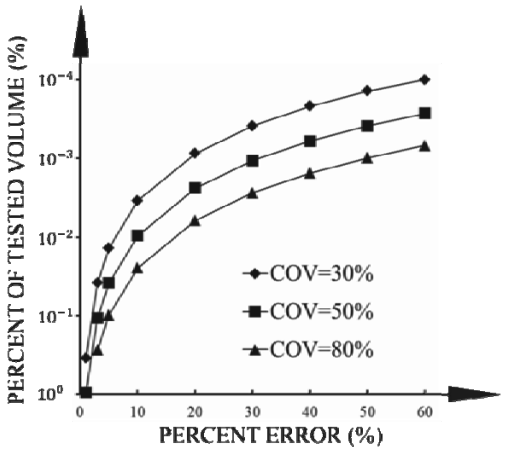

Figure 4. Required volume of soil to be tested as a percent of the total volume involved in the soil response to predict a soil property with a 98% confidence level and within a percent error for given coefficients of variation of the soil property.

Consider now an 8 story building which is 40 by 40 m at its base. The volume of soil involved in the response of the building to loading is at least 40 by 40 by 40 m or 64000 m^3. The required sampling is 0.001% or 0.64 m^3 which corresponds to 640 triaxial tests. Further assuming that we will drill 40 m deep borings allowing us to conduct 20 triaxial tests per boring, this would require some 32 borings. In practice, we would typically drill 4 or 5 borings for such a building. This shows that we do not test the soil enough in our current soil investigations to meet the set criterion. Note that the assumptions made in the student t distribution calculation include the assumption that the soil is uniformly variable. In other words, there are no heterogeneity trends or anomalies in the soil mass. If there were such anomalies, the amount of soil volume to test would increase. If we use the same approach for different volumes we can generate the number of borings necessary to meet the criterion of 98% confidence of predicting within + or – 20% for a soil with a coefficient of variation equal to 0.3. Fig. 5 shows the number of borings required as a function of the soil volume involved in the response to the loading. The estimated line for current practice is plotted on the same graph (based on the author's experience) indicating that current practice does not meet the criterion established. Note that the discrepancy increases with the size of the project. Indeed the ratio between the required number of borings N_r and the current number of borings N_c increases with the size of the imprint.

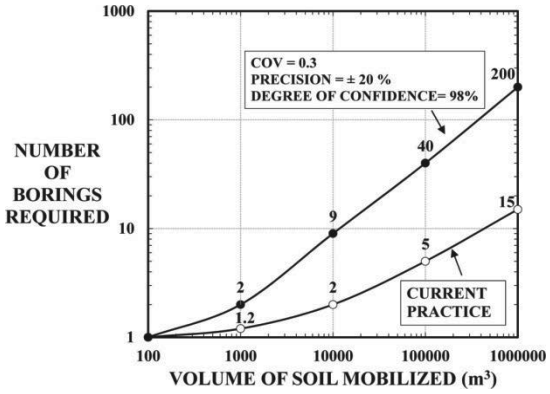

Figure 5. Comparison of number of borings in current practice and number of borings required for a precision of + or - 20% with a 98% degree of confidence for a soil parameter coefficient of variation of 0.3.

5 WHAT CAN BE IMPROVED ABOUT THE PMT EQUIPMENT?

Only a few things, I think. We are at the point of maturity in this area. If anything, we need to be able to run controlled stress tests or control strain tests equally well. Controlling strain or volume has the advantage of not having to guess at the limit pressure to decide on the pressure steps. Controlling pressure has the advantage of not having to wait for a long time if the hole is too big. The devices which control stress require compressed gas bottles which can be dangerous. Control volume devices are safer in that respect and still allow control stress tests. Most civil engineering structures apply stress control steps.

With regard to the issue of the three cells versus mono-cell probes, it has been shown (Briaud, 1992) that for probes with a length to diameter ratio longer than 6, the difference between the expansion of the mono-cell and the expansion of an infinitely long cylinder for an elastic soil are within 5 % of each other. Therefore as long as the probe has a length to diameter ratio of 6 or more, there is no need for three cells in a pressuremeter probe.

The diameter of the probe has an impact on the quality of the test for the following reason. The thickness of the ring of disturbed soil created by the carving or washing process during drilling is approximately constant regardless of the diameter of the drill bit. As such, the larger the pressuremeter diameter is, the less influence this disturbed zone will have on the pressuremeter curve. Therefore, it is best to increase the diameter of the pressuremeter probe. A larger diameter will also have a positive impact on the reliability of the borehole diameter as it is much easier to drill a well calibrated 150mm diameter hole than a 50mm diameter hole. Using lightweight yet rugged 150 mm diameter, 1 m long PMT probes will improve PMT test quality.

6 MAKING A QUALITY BOREHOLE IS THE MOST IMPORTANT STEP

This is the most important and the most difficult step in a quality pressuremeter test. Much has been tried and written on the best way to prepare the hole. Special training is required for drillers to prepare a good PMT borehole as drilling for PMT testing is very different and almost opposite to drilling for soil sampling (Table 1). Table 2 gives some general recommendations to obtain a quality borehole with wet rotary drilling which I would recommend in most cases.

Table 1. Differences between drilling for PMT testing and drilling for soil sampling

DRILLING FOR PMT TESTING	DRILLING FOR SAMPLING
Slow rotation to minimize enlargement of borehole diameter	Fast rotation to get to the sampling depth faster
Care about undisturbed borehole walls left behind the bit	Don't care about borehole walls left behind the bit
Don't care about soil in front of the bit	Care about undisturbed soil in front of the bit
Advance borehole beyond testing depth for cuttings to settle in	Stop at sampling depth
Do not clean the borehole by running the bit up and down in the open hole; this will increase the hole diameter	Clean borehole by running bit with fast mud flow up and down in open hole; avoids unwanted cuttings in sampling tube
Care about borehole diameter	Don't care about borehole diameter

Table 2. Recommendations for a quality PMT borehole by the wet rotary method.

Diameter of drilling bit should be equal to the diameter of the probe
Three wing bit for silts and clays (carving), roller bit for sands and gravels (washing)
Diameter of rods should be small enough to allow cuttings to go by
Slow rotation of the drill (60 rpm)
Slow mud circulation to minimize erosion
Drill 1 m past the testing depth for cuttings to settle
One pass down and one withdrawal (no cleaning of the hole)
One test at a time

7 THE PMT PARAMETERS

7.1 PMT Modulus and tension in the hoop direction

A number of parameters are obtained from the PMT. One of the most useful is the PMT modulus E_o from first loading This modulus is calculated by using the theory of elasticity. One of the assumptions in elasticity is that the soil has the same modulus in compression and in tension. This may be true to some extent for clays but unlikely true for sands. When the PMT probe expands, the radial stress increases and the hoop stress decreases to the point where it can reach tension. In elasticity, the increase in radial stress is equal to the decrease in hoop stress, so if the pressure in the PMT probe is 500 kPa, the hoop stress at the borehole wall is -500 kPa (neglecting the at rest pressure). The soil is unlikely to be able to resist such tension and using elasticity theory in this case is flawed. The following derivation shows the influence of having a much weaker modulus in tension than in compression.

The general orthotropic elastic equations are

$$\varepsilon_r = \frac{\sigma_r}{E_r} - \nu_{\theta r}\frac{\sigma_\theta}{E_\theta} - \nu_{zr}\frac{\sigma_z}{E_z} \tag{8}$$

$$\varepsilon_\theta = -\nu_{r\theta}\frac{\sigma_r}{E_r} + \frac{\sigma_\theta}{E_\theta} - \nu_{z\theta}\frac{\sigma_z}{E_z} \tag{9}$$

$$\varepsilon_z = -\nu_{rz}\frac{\sigma_r}{E_r} - \nu_{\theta z}\frac{\sigma_\theta}{E_\theta} + \frac{\sigma_z}{E_z} \tag{10}$$

Where ε_r, ε_θ, ε_z are the normal strains in the r, θ, and z directions, σ_r, σ_θ, σ_z are the normal stresses in the r, θ, and z directions, E_r, E_θ, E_z are the modulus in the r, θ, and z directions, and $\nu_{\theta r}$, $\nu_{r\theta}$, ν_{zr}, ν_{rz}, $\nu_{z\theta}$, $\nu_{\theta z}$ are the Poisson's ratios. Because of the symmetry rules, the following equations must also be satisfied

$$E_r\nu_{\theta r} = E_\theta\nu_{r\theta} \tag{11}$$

$$E_z\nu_{\theta z} = E_\theta\nu_{z\theta} \tag{12}$$

$$E_r\nu_{zr} = E_z\nu_{rz} \tag{13}$$

Here it is assumed that a compression modulus E^+ acts in the radial and vertical direction and a much reduced tension modulus E^- acts in the hoop direction.

$$E_z = E_r = E^+ \tag{14}$$

$$E_\theta = E^- \tag{15}$$

Where E^+ is the modulus of the soil when tested in compression and E^- is the modulus of the soil when tested in tension. The problem is further simplified by assuming that

$$\nu_{rz} = \nu_{zr} = \nu_1 \tag{16}$$

$$\nu_{\theta z} = \nu_{\theta r} = \nu_2 \tag{17}$$

$$\nu_{z\theta} = \nu_{r\theta} = \nu_3 \tag{18}$$

The plane strain condition of the cylindrical deformation gives

$$\varepsilon_z = 0 \tag{19}$$

The definition of the strains is, in small strain theory

$$\varepsilon_r = \frac{du}{dr} \tag{20}$$

$$\varepsilon_\theta = \frac{u}{r} \tag{21}$$

Now the equilibrium equation gives

$$\frac{d\sigma_r}{dr} + \frac{\sigma_r - \sigma_\theta}{r} = 0 \tag{22}$$

Using Eq. 8 to 22 leads to the governing differential equation where the displacement u is the variable. The boundary conditions are a displacement equal to zero for an infinite radius and a pressure equal to the imposed pressure at the cavity wall. The solution is a bit cumbersome:

$$\sigma_{ro} = \left(s_{12} - \frac{1}{2}\left((s_{21} - s_{12}) - \sqrt{(s_{21} - s_{12})^2 + 4s_{11}s_{22}}\right)\right)\frac{u_o}{r_o} \tag{23}$$

Where s_{11}, s_{22}, s_{12}, s_{21} are defined as follows

$$s_{11} = \frac{E^+\left(1-\nu_2^2\right)}{\left(1-2\nu_2^2-\nu_1\right)\left(1+\nu_1\right)} \tag{24}$$

$$s_{12} = \frac{E^+\nu_2}{\left(1-2\nu_2^2-\nu_1\right)} \tag{25}$$

$$s_{21} = \frac{E^-\nu_2}{\left(1-2\nu_2^2-\nu_1\right)} \tag{26}$$

$$s_{22} = \frac{E^-\left(1-\nu_1\right)}{\left(1-2\nu_2^2-\nu_1\right)} \tag{27}$$

Eq. 23 is to be compared with the equation for the isotropic solution which is

$$\sigma_{ro} = \left(\frac{E_o}{1+\nu}\right)\frac{u_o}{r_o} \tag{28}$$

Consider the case where the ratio E^+/E^- = 10, $\nu_1 = \nu_3 = 0.33$, then ν_2 equal to 0.033. Then Eq.23 and Eq. 28 give respectively:

$$\sigma_{ro} = 0.309E^+ \frac{u_o}{r_o} \quad (29)$$

$$\sigma_{ro} = 0.752E_o \frac{u_o}{r_o} \quad (30)$$

Therefore, $E^+ = 2.43E_o$ (31)

This can be repeated for different values of E^+/E^- to obtain Fig. 6. The inverse of the modulus ratio is consistent with the values recommended by Menard for the α values in settlement analysis as shown in Fig.6. This observation about the tension in the hoop direction also impacts PMT tests in hard soils and rock which are sound enough to exhibit significant tensile strength. In this case, the PMT curve shows a break in the expansion curve (Fig. 7) at a pressure p where the hard soil or rock breaks in tension. This pressure is such that (Briaud, 1992):

$$\sigma_t = p - 2\sigma_{oh} \quad (32)$$

Where σ_t is the soil tensile strength and σ_{oh} is the horizontal stress at rest before the PMT is inserted.

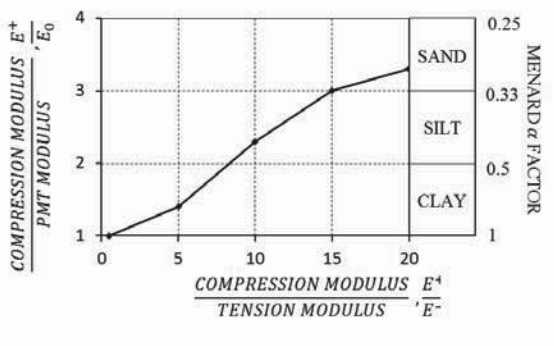

Figure 6. Correction of PMT modulus for low tension soils

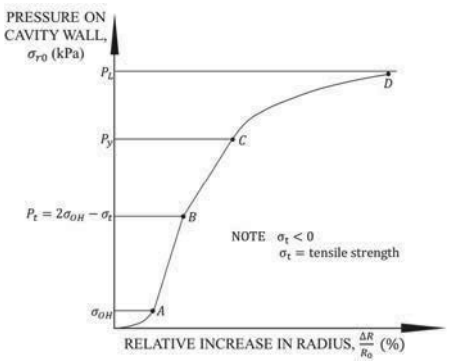

Figure 7. Tensile strength from PMT test

7.2 PMT first load modulus

The PMT first load modulus E_o also called the Menard modulus is obtained from the initial straight line part of the PMT curve. This straight line exists over a range of relative increase in cavity radius which varies from one soil to another but is typically in the range of 2 to 6 % relative increase in cavity radius. At two sites in Texas, one in stiff clay the other in dense sand, the average range of 15 PMT tests was 3.47% for the clay site and 3.59% for the sand site. This refers to the value of $\Delta R/R_o$ at the cavity wall. The average radial strain in the soil mass involved in the response to the cylindrical cavity expansion is much smaller and averages 0.316 $\Delta R/R_o$ as shown in the following. The hoop strain ε_θ and the increase in radial stress $\Delta\sigma_r$ decrease away from the wall of the cavity at a rate of $1/R^2$ where R is the radial distance into the soil mass (Baguelin et al., 1978). If the radius of influence of the pressuremeter expansion is defined as the radius at which ε_θ and $\Delta\sigma_r$ are $1/10^{th}$ of the value at the cavity wall, that radius of influence is $10^{0.5}R_o = 3.16R_o$. Within this radius of influence, the average strain ε_θ can be calculated as follows

$$\varepsilon_{\theta av} = \frac{1}{(3.16R_o - R_o)} \int_{R_o}^{3.16R_o} \frac{\varepsilon_{\theta o} R_o^2}{R^2} dR = 0.316\varepsilon_{\theta o} \quad (33)$$

where $\varepsilon_{\theta av}$ is the average hoop strain within the radius of influence of the pressuremeter test, $\varepsilon_{\theta o}$ is the hoop strain at the wall of the cavity, R_o is the initial radius of the cavity, and R is the radial distance in the soil. The modulus was mentioned as being associated with a strain level at the cavity wall $\varepsilon_{\theta o}$ typically in the range of 2 to 6%; this means that the average strain $\varepsilon_{\theta av}$ will be 0.6 to 2%. For the two Texas sites mentioned above, the average strain would be close to 1% (3.53% x 0.316). Note that this range of strain is consistent with the strain level associated with foundation engineering but is much higher than the range of strain associated with pavement design or earthquake shaking where a very low strain modulus is used.

The fact that the small strain modulus is absent from the beginning of the PMT curve and that the strain range is between 0.6 to 2%, is created in part by the recompression of the soil which was decompressed horizontally by the drilling process. This recompression makes the small strain part of the stress strain curve disappear as shown in the PMT test on Fig. 8. In this test, an unload-reload loop was performed by decreasing the pressure to zero and increasing it again to simulate a first expansion curve. Then a second unload-reload loop was performed over a much smaller pressure range. This test shows that the recompression modulus varies tremendously depending on the extent of the unloading. This test also shows that the low strain information is lost in the decompression and recompression loading process. Can we find a way to recreate the early part of the PMT curve from the information gathered during the test.

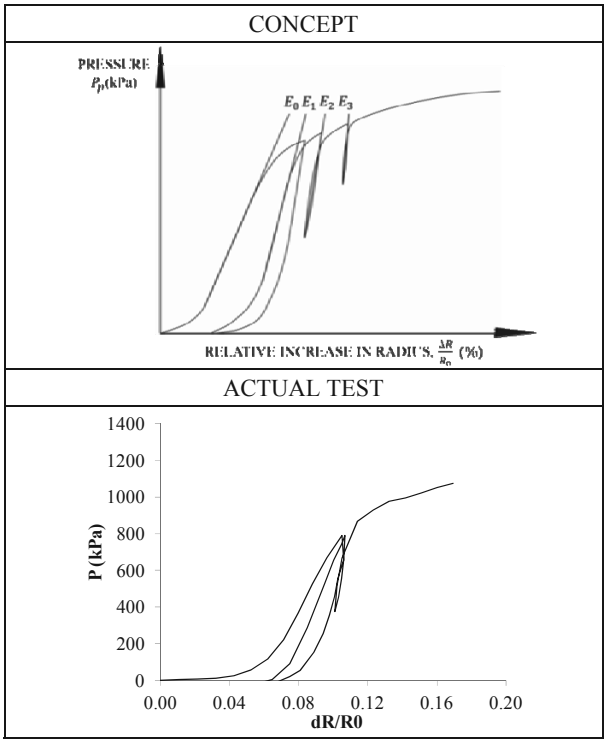

Figure 8. PMT stress strain curve with unload reload loops

7.3 PMT modulus at small strain

A soil modulus depends on several factors (Briaud, 2013) one of which is the strain level. The PMT curve is a stress strain curve where the stress is the radial stress σ_r (measured pressure

in the PMT) and the strain is the hoop strain ε_θ (relative increase in cavity radius). It is therefore possible to define a secant modulus as a function of strain from the PMT curve (Fig. 9).

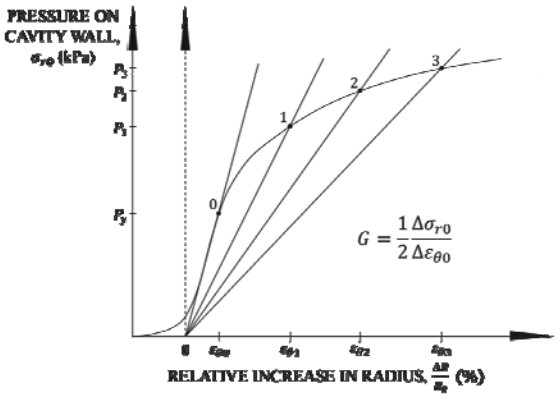

Figure 9. PMT stress strain curve and secant modulus

It can be shown in elasticity that the shear modulus is given by:

$$G = \frac{1}{2}\frac{\Delta\sigma_{ro}}{\Delta\varepsilon_{\theta o}} \tag{34}$$

If we call G_o the shear modulus associated with the straight portion of the curve, we can normalize the modulus at any strain with respect to G_o. We calculate the secant shear modulus G_1, G_2, G_3 and so on corresponding to points 1, 2, and 3 on the pressuremeter curve (Fig. 9). Then we can plot the ratio G_1/G_o, G_2/G_o, G_3/G_o as a function of the corresponding strain $\varepsilon_{\theta 1}$, $\varepsilon_{\theta 2}$, $\varepsilon_{\theta 3}$. Note that ε_θ is the strain at the cavity wall but that the mean strain $\varepsilon_{\theta mean}$ induced in the soil within the zone of influence is only about 32% of that value (Eq. 33).

The curve linking G/G_o vs. $\varepsilon_{\theta mean}$ is shown on Fig. 10c and 10d. From zero strain to the strain value corresponding to the end of the straight part of the PMT curve (AB on Fig. 10a), the G/G_o vs. $\varepsilon_{\theta mean}$ curve is flat on Fig. 10c and 10d because within that strain range the modulus G is constant and equal to G_o.

In order to generate the non linear beginning of that curve (EB on Fig. 10a), it is convenient to assume a hyperbolic model as proposed by Baud et al. (2013) of the form

$$\sigma = \frac{\varepsilon}{\frac{1}{2G_{max}} + \frac{\varepsilon}{p_L}} \tag{35}$$

This equation defines a hyperbola which describes the PMT curve with the limit pressure p_L as the asymptotic value and $2G_{max}$ as the initial tangent modulus. The hyperbolic model has been shown to be very successful in describing the stress strain curve of soils (Duncan, Chang, 1970). In Eq. 35, p_L is known and all the points on the PMT curve, after excluding the points on the straight line part, can be used to find the optimum value of G_{max} by best fit regression. This can be done by plotting the data points as ε/σ vs. ε and fitting a straight line through the data points (Fig. 10b). Then $1/2G_{max}$ is the ordinate at $\varepsilon = 0$ and $1/p_L$ is the slope of the line.

$$\frac{\varepsilon}{\sigma} = \frac{1}{2G_{max}} + \frac{\varepsilon}{p_L} \tag{36}$$

Then Eq. 35 gives the complete curve. This technique was used at two sites, a stiff clay site near Houston, Texas, and a medium dense sand site in Corpus Christi, Texas. Example results are presented in Fig. 11 which shows that the data fits well with a hyperbolic equation. For these two sites, the average ratio G_{max}/G_o was 1.75 for the stiff clay and 1.27 for the dense sand.

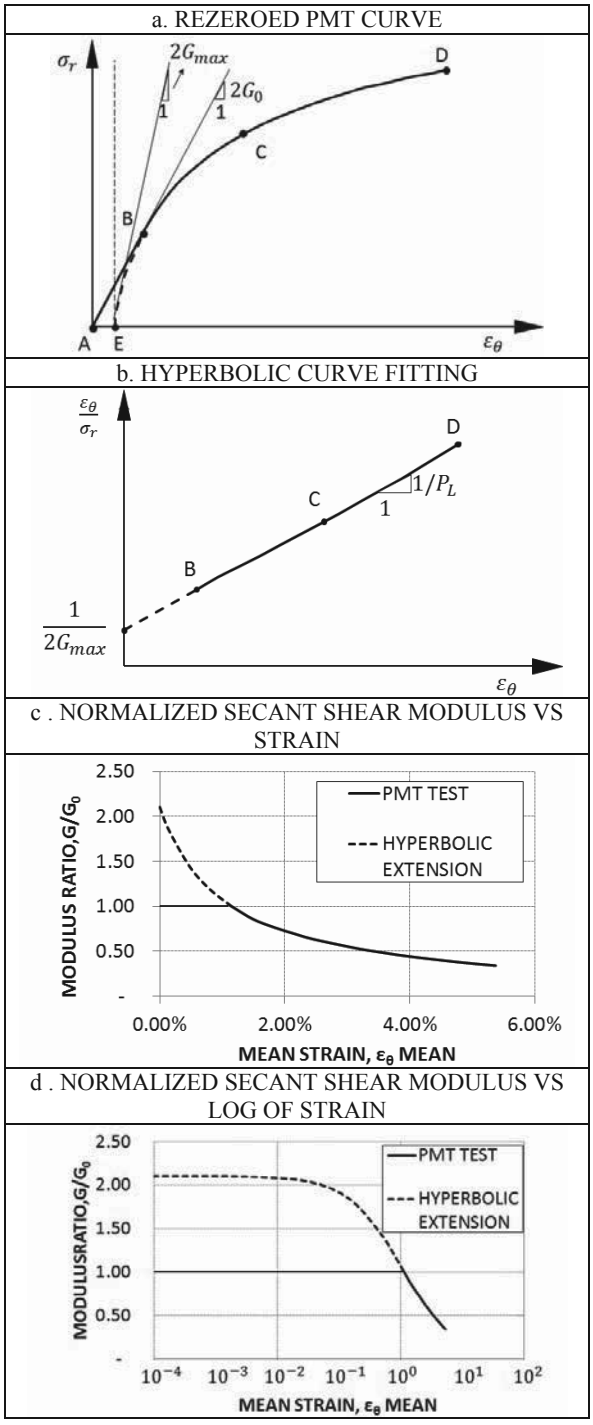

Figure 10. Normalized secant shear modulus vs. strain

Estimates of G_{max} were calculated independently by using correlations proposed by Seed et al. (1986) based on SPT blow count for sand, Rix and Stokoe (1991) based on CPT point resistance for sand, and Mayne and Rix (1993) based on CPT point resistance and void ratio for clays. These estimates of G_{max} were consistently much higher than the values obtained by the hyperbolic extension of the PMT curve; 25 times larger for the stiff clay and 44 times larger for the dense sand. This indicates that this hyperbolic fit to the PMT curve does not lead to accurate very small strain moduli.

a. PMT CURVE – STIFF CLAY

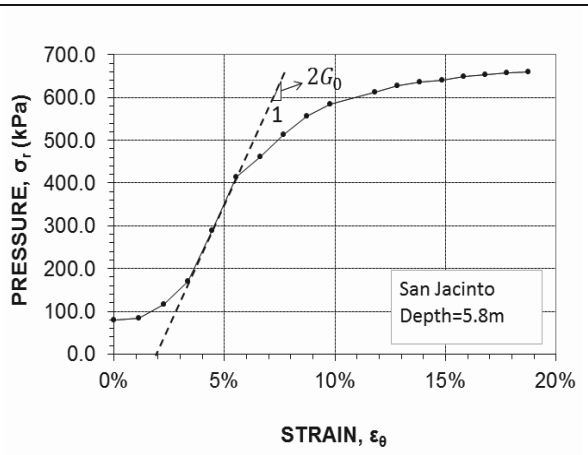

b. HYPERBOLIC CURVE FITTING

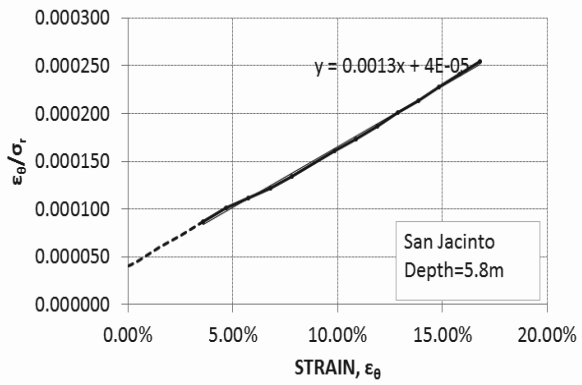

c. NORMALIZED SECANT SHEAR MODULUS VS STRAIN

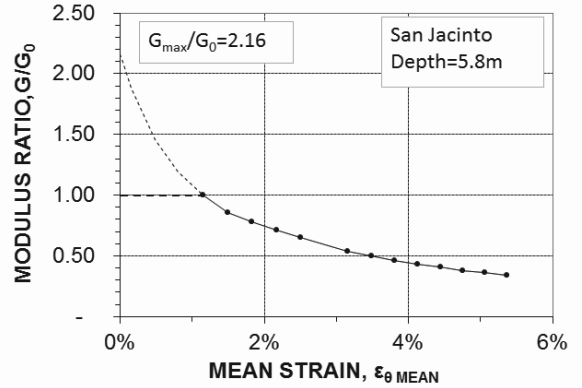

d. NORMALIZED SHEAR MODULUS VS LOG STRAIN

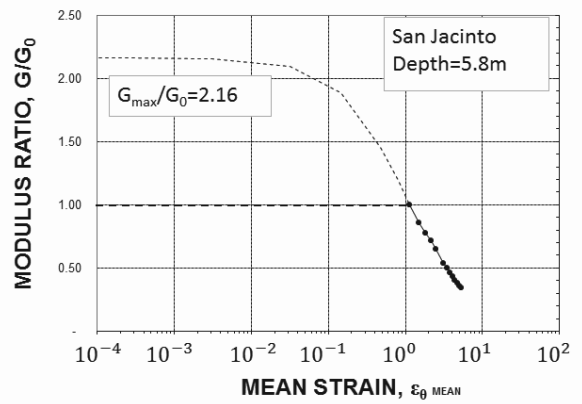

e. PMT CURVE – DENSE SAND

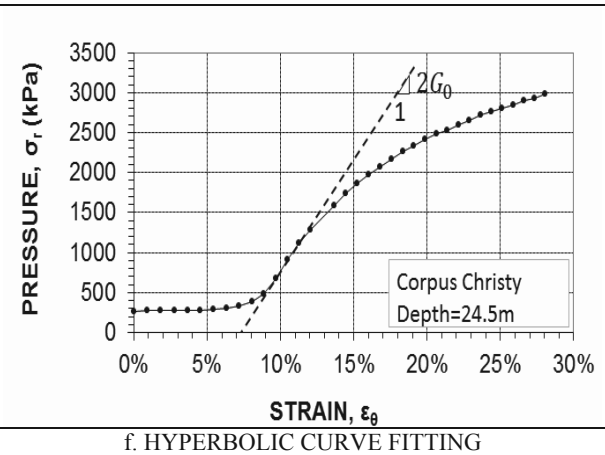

f. HYPERBOLIC CURVE FITTING

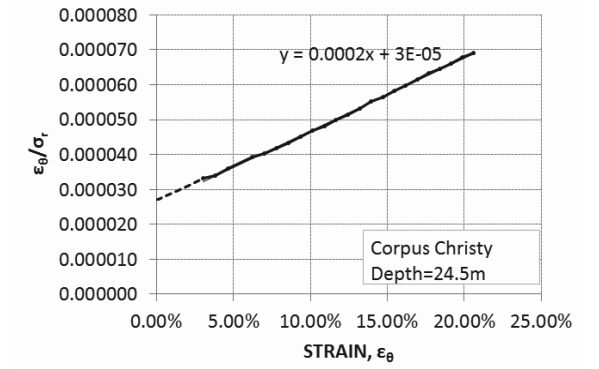

g. NORMALIZED SECANT SHEAR MODULUS VS STRAIN

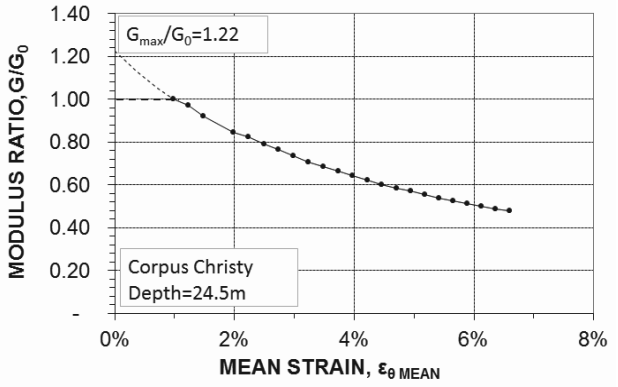

h. NORMALIZED SHEAR MODULUS VS LOG STRAIN

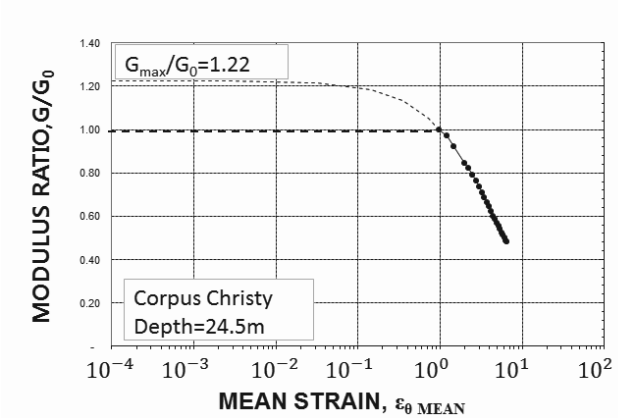

Figure 11. Examples of hyperbolic extension of the PMT curve (stiff clay, dense sand)

7.4 PMT modulus long term creep, and cyclic loading

It is relatively easy to maintain the pressure constant during a PMT test while recording the increase in radius of the cavity (Fig. 12). A pressure holding step of 10 minutes is not very time consuming and can lead to very valuable information if the structure will be subjected to long term loading (e.g.: building, retaining wall). The pressure held for 10 minutes should be higher than $0.2p_L$ because below that threshold the influence of the decompression-recompression effect and the disturbance effect is more pronounced (Briaud, 1992). The evolution of the secant modulus E_t during the pressure holding test is well described by the following model:

$$E_t = E_{t_o}\left(\frac{t}{t_o}\right)^{-n} \quad (37)$$

Where t is the time after the start of the pressure holding step, t_o is a reference time after the start of the pressure holding step usually taken as 1 minute, E_t and E_{to} are the secant modulus corresponding to t and t_o respectively, and n is the creep exponent. The value of n is obtained as the slope of the plot of log E_t/E_{to} vs. log t/t_o. The creep exponent n increases with the stress applied over strength ratio and depends on the soil type and stress history. It has been found in the range of 0.01 to 0.03 for sands and in the rnage of 0.03 to 0.08 for clays (Briaud, 1992). For clays, the lower values are for overconsolidated clays while the higher values are for very soft clays. Measurements on large scale spread footings on an unsaturated silty sand (Briaud, Gibbens, 1999) demonstrated that the power law model works very well (Fig. 13) because the log settlement vs. log time curve was remarkably linear. These experiments also indicated that n increases with the load level but is significantly reduced by unload reload cycles. PMT tests with creep steps were performed next to the footings (Fig. 13c and 13d); the parallel between the footing and the PMT is striking.

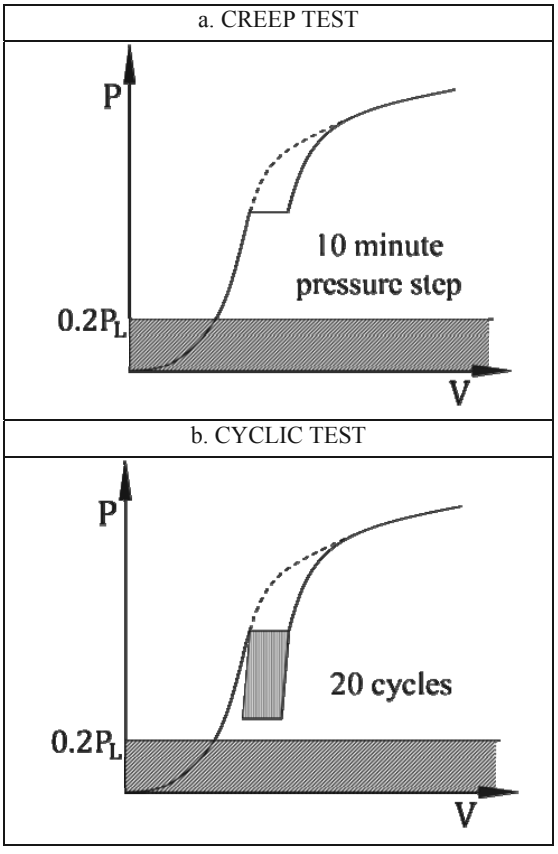

Figure 12. Creep and cyclic PMT test

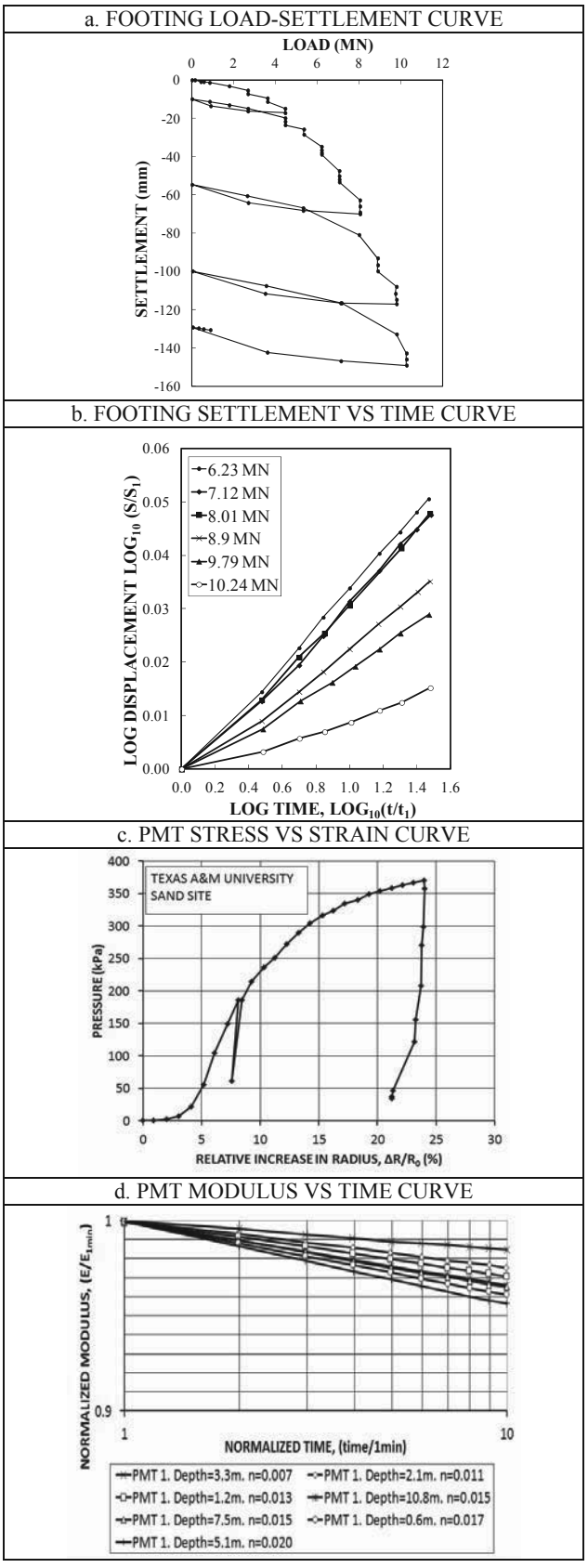

Figure 13. Creep response of a 3m by 3m spread footing and a PMT test (Briaud, Gibbens, 1999, Jeanjean, 1995).

Similarly, one can conduct cyclic loading during the PMT test. A series of 10 cycles is not very time consuming and can lead to very valuable information if the structure will be

subjected to significant repeated loading (e.g.: large wave loading). The evolution of the secant modulus E_N to the top of cycle N is well described by the following model

$$E_N = E_1 N^{-m} \quad (38)$$

Where N is the number of cycle using number 1 as the first loading cycle, E_N the secant modulus to the top of the N^{th} cycle, E_1 the secant modulus to the top of the first cycle (first time that the pressure is decreased), and m is the cyclic exponent. The value of m is obtained as the slope of the plot of log E_N/E_1 vs. log N. Fig. 14 shows a parallel example of a pile subjected to cyclic horizontal loading and a cyclic PMT test. As can be seen the power law model of Eq.38 describes the evolution of the deformation with the number of cycles (straight line on log-log scales) very well and the parallel between the pile and the PMT is striking.

7.5 PMT unload-reload modulus

The unload reload modulus E_r is obtained by performing an unload reload loop during the PMT test. The main problem with E_r is that, unlike E_o, it is not precisely defined. Indeed it depends on the strain amplitude over which the loop is performed and to a lesser extent on the stress level at which the loop is performed. As such, E_r varies widely from one user to another and cannot be relied upon for standard calculations unless the strain amplitude and stress level have been selected to match the problem at hand. In my practice, I perform an unload reload loop at the end of the linear phase and unload until the pressure has reached one half of the peak pressure. This has the advantage of being consistent but does not necessarily correspond to a consistent strain amplitude from one test to the next. I would strongly discourage the use of the reload modulus because it is not a standard modulus. Instead I would recommend the use of a hyperbolic extension of the PMT curve to find the modulus at the right strain level.

7.6 The yield pressure p_y.

The yield pressure p_y is found at the end of the straight line corresponding to the PMT modulus. Up to p_y, the amount of creep is reasonably small but becomes much larger beyond that. In geotechnical engineering it is always desirable to apply pressures on the soil below the value of p_y. Typically p_y is 0.5 p_L for clays and 0.33 p_L for sands. Therefore, at working loads, it is advisable to keep the pressure under foundations at most equal to 0.5 p_L in clays and 0.33 p_L in sands to limit creep deformations.

7.7 Correlations between PMT parameters and other soil parameters

Correlations based on 426 PMT tests performed at 36 sites in sand and 44 sites in clay along with other measured soil parameters were presented by Briaud (1992). These correlations exhibit significant scatter and should be used with caution. Nevertheless they are very useful in preliminary calculations and for estimate purposes. Table 3 gives the range of expected PMT limit pressure and modulus in various soils while Tables 4 and 5 give the correlations.

Table 3. Expected values of E_o and P_L in soils

CLAY					
Soil strength	Soft	Medium	Stiff	Very Stiff	Hard
p^*_L(kPa)	0–200	200–400	400–800	800-1600	>1600
E_0 (MPa)	0 – 2.5	2.5 - 5.0	5.0 - 12	12 - 25	> 25
SAND					
Soil strength	Loose	Compact	Dense	Very Dense	
p^*_L(kPa)	0 – 500	500 - 1500	1500-2500	> 2500	
E_0(MPa)	0 – 3.5	3.5 - 12	12 – 22.5	> 22.5	

a. PILE LOAD-DISPLACEMENT CURVE

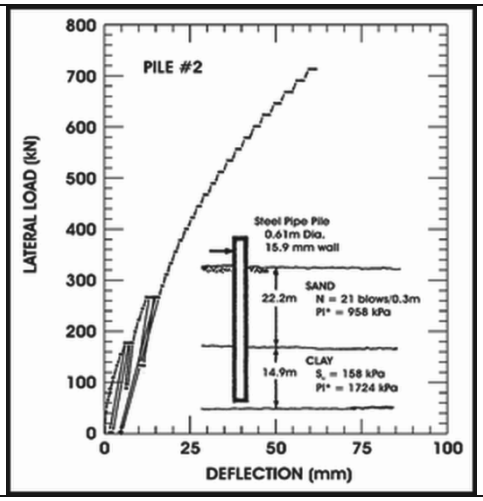

b. PILE STIFFNESS VS NUMBER OF CYCLES CURVE

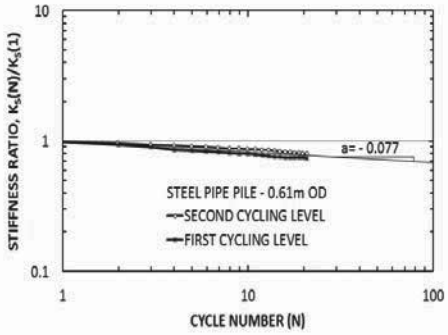

c. PMT STRESS STRAIN CURVE

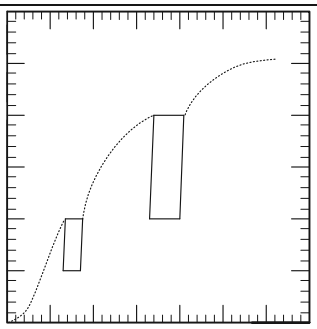

d. PMT MODULUS VS NUMBER OF CYCLES CURVE

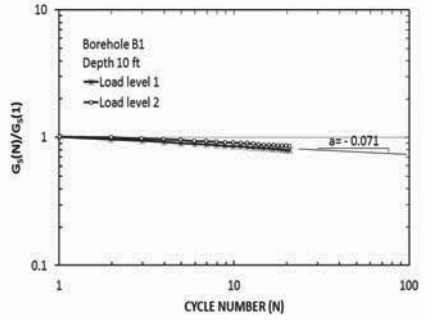

Figure 14. Cyclic response of a laterally loaded pile A and a PMT test (Little, Briaud, 1988).

Table 4. Correlations for Sand (Column A = Number in Table x Row B)

Column A = number in table x row B						
B A	E_0 (kPa)	E_R (kPa)	p^*_L (kPa)	q_c (kPa)	f_s (kPa)	N (bpf)
E_0 (kPa)	1	0.125	8	1.15	57.5	383
E_R (kPa)	8	1	64	6.25	312.5	2174
p^*_L (kPa)	0.125	0.0156	1	0.11	5.5	47.9
q_c (kPa)	0.87	0.16	9	1	50	436
f_s (kPa)	0.0174	0.0032	0.182	0.02	1	9.58
N (bpf)	0.0026	0.00046	0.021	0.0021	0.104	1

Table 5. Correlations for Clay (Column A = Number in Table x Row B)

Column A = number in table x row B							
B A	E_0 (kPa)	E_R (kPa)	p^*_L (kPa)	q_c (kPa)	f_s (kPa)	s_u (kPa)	N (bpf)
E_0 (kPa)	1	0.278	14	2.5	56	100	667
E_R (kPa)	3.6	1	50	13	260	300	2000
p^*_L (kPa)	0.071	0.02	1	0.2	4	7.5	50
q_c (kPa)	0.40	0.077	5	1	20	27	180
f_s (kPa)	0.079	0.0038	0.25	0.05	1	1.6	10.7
s_u (kPa)	0.010	0.0033	0.133	0.037	0.625	1	6.7
N (bpf)	0.0015	0.0005	0.02	0.0056	0.091	0.14	1

8 SHALLOW FOUNDATIONS

8.1 Ultimate bearing capacity

The general bearing capacity equation for a strip footing is:

$$p_u = c' N_c + \frac{1}{2}\gamma B N_\gamma + \gamma D N_q \quad (39)$$

Where p_u is the ultimate bearing pressure, c' the effective stress cohesion intercept, γ the effective unit weight of the soil, N_c, N_γ, and N_q bearing capacity factors depending on the friction angle φ'. The assumptions made to develop this equation include that the unit weight and the friction angle of the soil are constant. Therefore the strength profile of the soil is linearly increasing with depth. For strength profiles which do not increase linearly with depth, this equation does not work and can severely overestimate the value of p_u. However equations of the following form always take into account the proper soil strength:

$$p_u = k\, s + \gamma\, D \quad (40)$$

Where k is a bearing capacity factor, s is a strength parameter for the soil, γ is the unit weight of the soil, and D is the depth of embedment. The parameter s can be the PMT limit pressure p_L, the CPT point resistance q_c, or the SPT blow count N. Table 6 gives the values of k for various soils and various tests in the case of a horizontal square foundation on horizontal flat ground under axial vertical load.

Table 6. Bearing capacity factors k for in situ tests

Strength parameter	Clay	Sand
PMT p_L(kPa)	1.25	1.7
CPT q_c(kPa)	0.3	0.2
SPT N(bpf)*	60	75

* Ultimate bearing capacity p_u in kPa.

8.2 Load settlement curve method for footings on sand

The typical approach in the design of shallow foundations is to calculate the ultimate bearing capacity p_u, reduce that pressure to a safe pressure p_{safe} by applying a combined load and resistance factor, use that safe pressure to calculate the corresponding settlement, compare that settlement to the allowable settlement, and adjust the footing size until both the ultimate limit state and the serviceability limit state are satisfied. In other words the design of shallow foundations defines two points on the load settlement curve: one for the ultimate load and one for the service load. It would be more convenient if the entire load settlement curve could be generated. Then the engineer could decide where, on that curve, the foundation should operate. This was the incentive to develop the load settlement curve method (Briaud, 2007).

Five very large spread footings on sand up to 3m x 3m in size were loaded up to 12 MN at the Texas A&M University National Geotechnical Experimentation Site (Fig. 15a). Inclinometer casings were installed at the edge of the footings as part of the instrumentation. They were read at various loads during the test and indicated that the soil was deforming in a barrel like shape (Fig. 15b). This is the reason why the pressuremeter curve was thought to be a good candidate to generate the load settlement curve for the footing. Note that, during these tests, the inclinometers never showed the type of wedge failure assumed in the general bearing capacity equation. It is reasonned that the footings were not pushed to sufficient penetration to generate this type of failure mechanism.

The transformation required a correspondence principle between a point on the pressuremeter curve and a point on the footing load settlement curve (Fig. 16). This correspondence was established on the basis of two equations: the first one would satisfy average strain compatibility between the two loading processes and the second one would transform the PMT pressure into the footing pressure for corresponding average strains. These equations are:

$$\frac{s}{B} = 0.24\frac{\Delta R}{R_o} \quad (41)$$

$$p_f = f_{L/B} f_e f_\delta f_{\beta,d} \Gamma p_p \quad (42)$$

Where s if the footing settlement, B the footing width, $\Delta R/R_o$ the relative increase in cavity radius in the PMT test, p_f the average pressure under the footing for a settlement s, $f_{L/B}$, f_e, f_δ, $f_{\beta,d}$ the correction factors to take into account the shape of the footing, the eccentricity of the load, the inclination of the load, and the proximity of a slope respectively, Γ a function of s/B, and p_p the pressuremeter pressure corresponding to $\Delta R/R_o$. The Γ function was originally obtained from the large scale footing load tests on sand at Texas A&M University (Jeanjean, 1995, Briaud, 2007) and then supplemented with other load tests. This led to the data shown on Fig. 17. Using all the curves (Fig. 17a), a mean and a design Γ function were obtained (Fig. 17b). The design Γ function curve is the mean Γ function curve minus one standard deviation.

The f correction factors have been determined through a series of numerical simulations previously calibrated against the large scale loading tests (Hossain, 1996, Briaud, 2007). Their expressions are as follows

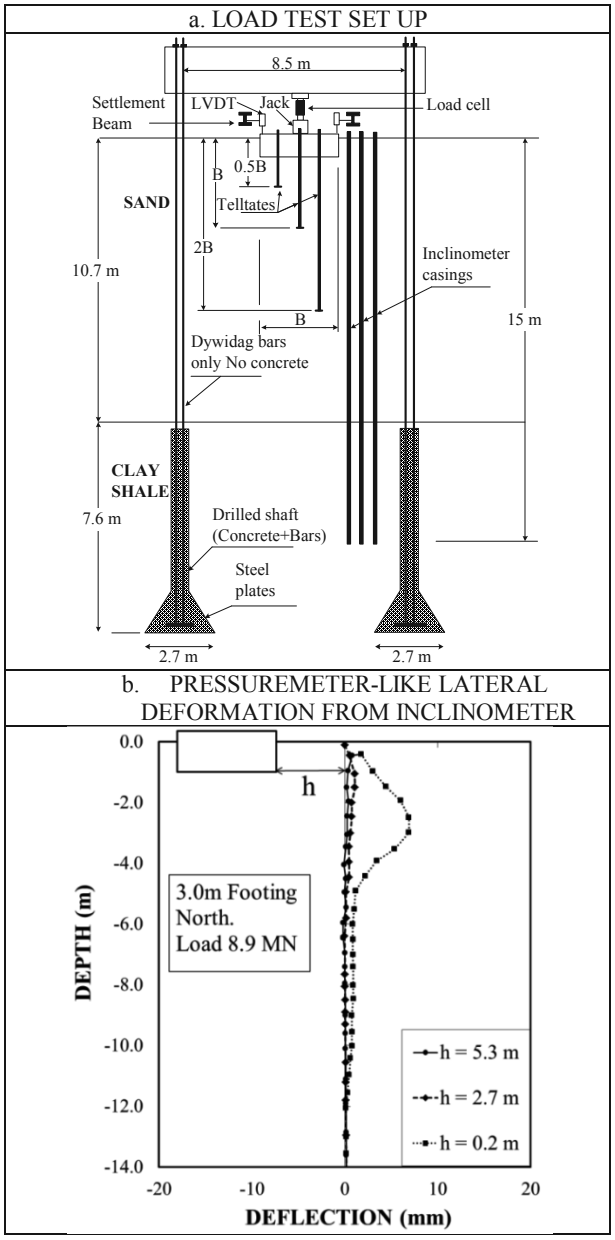

Figure 15. Analogy between the soil deformation under a shallow foundation and around a pressuremeter expansion test

Shape $$f_{L/B} = 0.8 + 0.2\frac{B}{L} \quad (43)$$

Eccentricity $$f_e = 1 - 0.33\frac{e}{B} \quad \text{center} \quad (44)$$

Eccentricity $$f_e = 1 - \left(\frac{e}{B}\right)^{0.5} \quad \text{edge} \quad (45)$$

Inclination $$f_\delta = 1 - \left(\frac{\delta}{90}\right)^2 \quad \text{center} \quad (46)$$

Inclination $$f_\delta = 1 - \left(\frac{\delta}{360}\right)^{0.5} \quad \text{edge} \quad (47)$$

Near 3/1 slope $$f_{\beta,d} = 0.8\left(1 + \frac{d}{B}\right)^{0.1} \quad (48)$$

Near 2/1 slope $$f_{\beta,d} = 0.7\left(1 + \frac{d}{B}\right)^{0.15} \quad (49)$$

Where B is the width of the footing, L its length, e the load eccentricity, δ the load inclination in degrees, and d the horizontal distance from the slope-side edge of the footing to the slope crest.

The shape of the Γ function indicates that at larger strain levels the need to correct the PMT curve is minimal. Indeed for s/B larger than 0.03, the mean value of Γ is constant and equal to about 1.5. For values of s/B smaller than 0.03, there is a need to correct the value of the PMT pressure because of a lack of curvature on the PMT curve compared to the curvature on the footing load settlement curve.

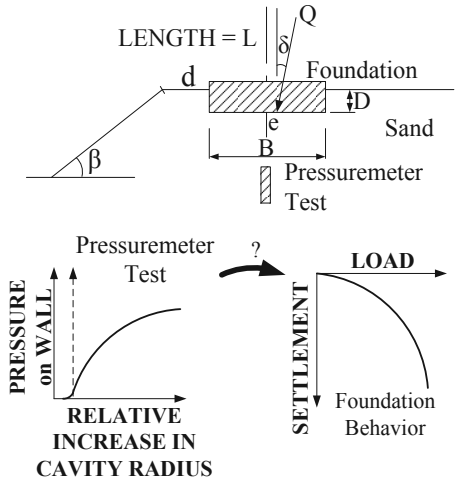

Figure 16. Transformation of the pressuremeter curve into the footing load settlement curve

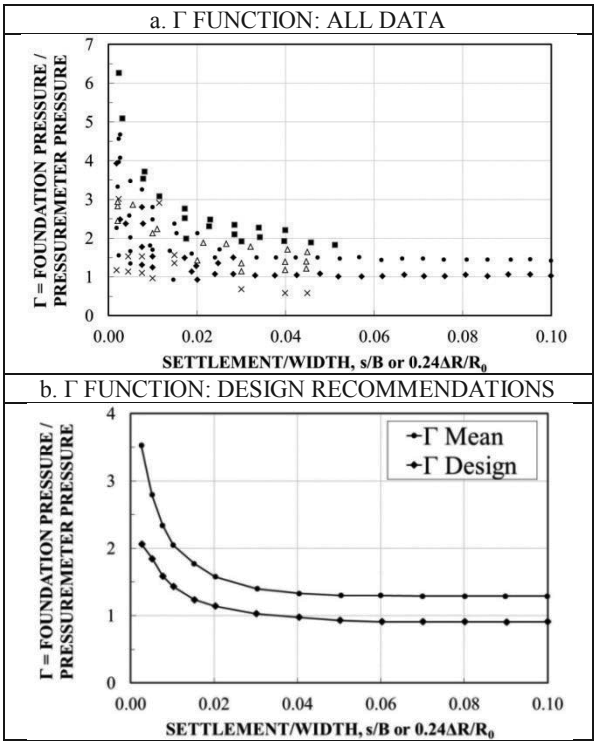

Figure 17. The Γ function for the load settlement curve method (Briaud 2013)

8.3 Load settlement curve method for footings on stiff clay

The load settlement curve method developed for sand was extended to stiff clay by using some footing load tests and parallel PMT tests. O'Neill and Sheikh (1985) load tested a 2.4 m diameter bored and under-reamed pile in Houston (Fig. 18a). The pile was 2.4 m deep (relative embedment depth D/B = 1) and the shaft friction was disabled by a casing. The soil was a stiff clay with an undrained shear strength of about 100 kPa. The load was increased in equal load steps and the resulting load settlement curve is shown in Fig. 18b. At failure, the average pressure under the footing was 680 kPa as measured by pressure cells on the bottom of the under-ream. Briaud et al. (1985) performed pressuremeter tests at the same site around the same time. The PMT test was carried out at a depth of 3.6 m or half a diameter below the bottom of the footing; this PMT curve (Fig.19a) was used to generate the Γ function for that stiff clay (Fig. 19b). As can be seen, the curve for that stiff clay is very close to the recommended mean curve for sand. Load tests on stiff clay using a 0.76m diameter plate at a depth of 1.52m (Tand, 2013) were also analyzed together with parallel PMT tests (Briaud, 1985) and gave the other Γ functions on Fig.19b. These tests on stiff clay give an indication that the design Γ function of Fig. 17b is equally applicable to sands and stiff clays. Note that the load settlement curve method gives the response of the footing as measured in load tests. These load tests are carried out in a few hours; if the loading time is very different (one week or more or one second or less), the time effect must be considered separately (Section 7.4).

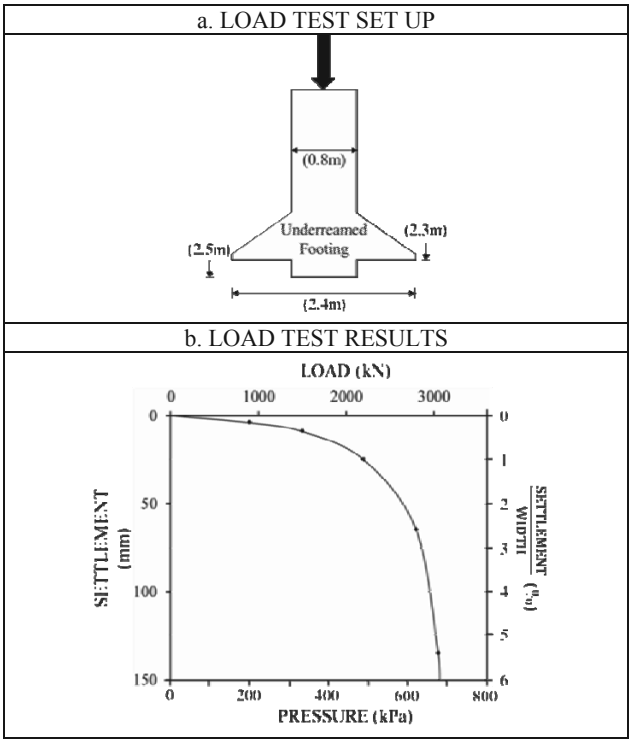

Figure 18. Large scale footing load test in stiff clay in Houston (O'Neill, Sheikh, 1985)

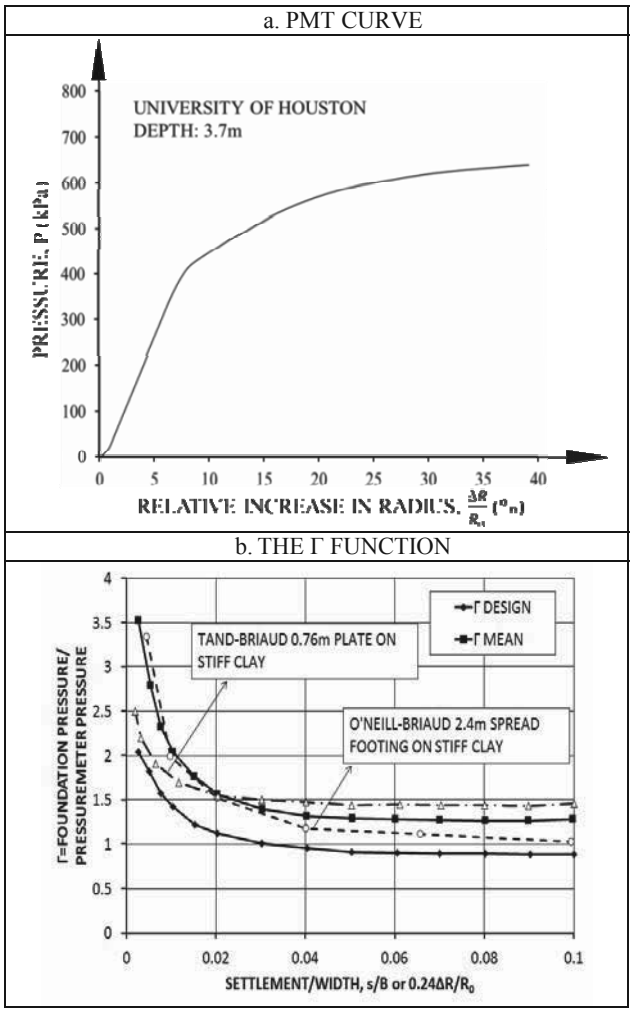

Figure 19. Pressuremeter test (Briaud et al, 1985) and Γ function for stiff clay

9 DEEP FOUNDATIONS UNDER VERTICAL LOADS

The rules developed by the French administration (Fascicule 62, 1993) for calculating the vertical capacity of piles are based on a very impressive database of load tests carried out by Bustamante and Gianeselli and the Laboratoires des Ponts et Chaussees from about 1975 to 1995. These rules were recently updated (NF P94-262, 2012) and represent one of the most complete and detailed axial capacity methodology in existence. These rules should be followed closely as there is no viable alternative for the PMT.

One area of deep foundations where the pressuremeter has seen some expanded use is the foundation design of very tall buildings such as the 452 m high Petronas Towers in Kuala Lumpur, Malaysia (Baker, 2010), the 828 m high Burj Khalifa in Dubai, UAE (Poulos 2009), the planned 1000 m high Nakheel Tower in Dubai, UAE (Haberfield, Paul, 2010), and the planned 1000m+ Kingdom Tower in Jeddah, Saudi Arabia (Poeppel, 2013). It is also seeing increased use for very large foundations such as the I10/I19 freeway interchange in Tucson, USA (Samtani, Liu, 2005). The use of the PMT for very tall buildings started with the work of Clyde Baker between 1965 and 1985 (Baker, 2005) for the Chicago high-rises where the use of the pressuremeter in the glacial till allowed Clyde Baker to increase the allowable pressure at the bottom of bored piles from 1.4 MPa to 2.4 MPa. The 1.4 MPa value was based on unconfined compression tests; the use of the pressuremeter along with observations led to using the 2.4 MPa value as confidence was gained.

In making settlement calculations for such structures, some use the rules proposed by Menard and some use the elastic equations often with an unload-reload modulus. Those who use the Menard rules, use α values based on local experience and influenced by the ratio between the unload-reload modulus E_r and the first load modulus E_o. While the value of the ratio E_o/E_r varies within a range somewhat similar to the range of α values, it is not clear why one should be related to the other. The ratio E_o/E_r is influenced by the development of plastic deformation around the probe while the value of α is argued to be related to the combination of lack of strength in tension (hoop direction as shown in Section 7.1) and recompression process through an S shape curve (Fig. 8). Those who use the elastic equation together with an unload-reload modulus face the problem that the unload reload modulus is ill defined and depends in particular on the extent of the unloading and the stress level at which the unloading takes place.

The case of the foundation of the tallest tower on Earth, the 828m high Burj Khalifa in Dubai, UAE, is studied further to investigate the issue of the first load modulus and the reload modulus (Poulos, 2009). The Burj Khalifa weighs approximately 5000MN and has a foundation imprint of about 3300m^2. The foundation is a combined pile raft 3.5 m thick founded at a depth of about 10 m below ground level on 1.5 m diameter bored piles extending some 50 m below the raft. To predict the settlement of the tower, a number of methods were used including numerical simulations. For these simulations a modulus profile was selected from all soil data available including 40 PMT tests. The PMT first load modulus profile is shown in Fig. 20 along with the selected design profile as input for settlement calculations by numerical simulations. As can be seen the design profile splits the PMT first load modulus profile with some conservatism. The settlement of the tower was predicted to be 77mm; it was measured during construction and reached 45 mm at the end of construction (Fig. 21). The reasonable comparison between measured and predicted settlement for this major case history gives an indication that it is appropriate to use the PMT first load modulus for settlement estimates.

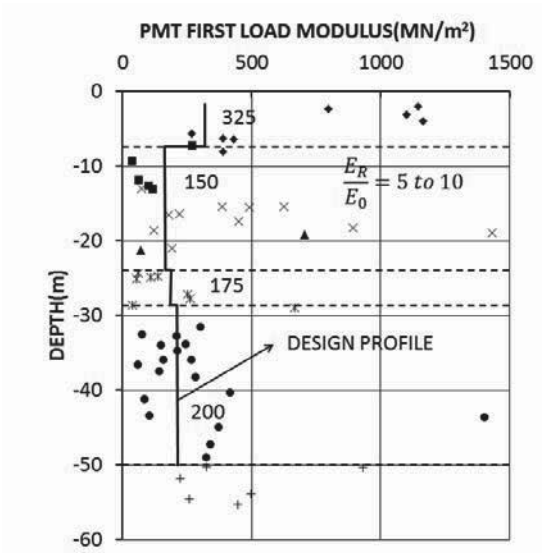

Figure 20. First load PMT modulus profile and selected design modulus values for the Burj Khalifa, Dubai, UAE (after Poulos, 2009)

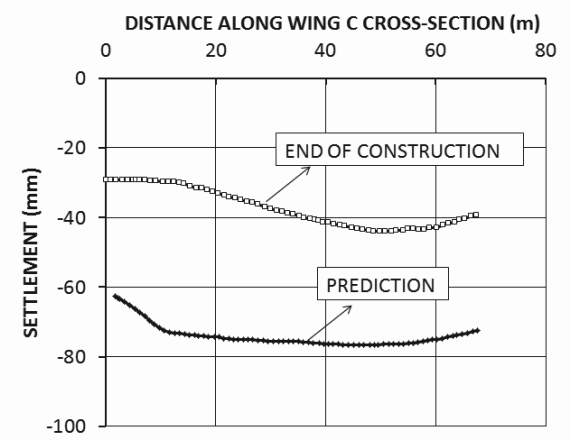

Figure 21. Measured and predicted settlement of the Burj Khalifa, Dubai, UAE (after Poulos, 2009)

10 DEEP FOUNDATIONS UNDER HORIZONTAL LOADS

10.1 Single pile behavior

For vertically loaded piles, it is common to calculate the ultimate capacity of the pile due to soil failure and then the settlement at working load. For horizontally loaded piles, an ultimate load due to soil failure is not usually calculated. Briaud (1997) proposed an equation to calculate the ultimate horizontal load due to soil failure for a horizontally loaded pile.

$$H_{ou} = \frac{3}{4} p_L B D_v \quad \begin{cases} D_v = \left(\frac{\pi}{4}\right) l_o \quad for \quad L > 3l_o \\ D_v = \frac{L}{3} \quad for \quad L < l_o \\ l_o = \left(\frac{4E_p I}{K}\right)^{1/4} \\ K = 2.3E_o \end{cases} \tag{50}$$

Where H_{ou} is the horizontal load corresponding to a horizontal displacement equal to 0.1B, B the pile diameter, p_L the PMT limit pressure, D_v the depth corresponding to zero shear force and maximum bending moment, l_o the transfer length, L the pile length, E_p the modulus of the pile material, I the moment of inertia of the pile around the bending axis, K the soil stiffness, and E_o the PMT first load modulus.

In order to expand that solution to create the entire load displacement curve for horizontally loaded piles, it is proposed to first use a strain compatibility equation such that the relative displacement to reach the ultimate load on the pile (y/B = 0.1) corresponds to the relative PMT expansion at the limit pressure ($\Delta R/R_o = 0.41$).

$$\frac{y}{B} = 0.24 \frac{\Delta R}{R_o} \tag{51}$$

Then the load on the pile can be transformed into a pressure within the most contributing zone as

$$p_{pile} = \frac{H_o}{BD_v} \tag{52}$$

The Γ value is the ratio of the pressure on the pile divided by the pressure on the PMT for a corresponding set of values of y/B and $\Delta R/R_o$ which satisfy Eq. 51. That way and point by point, the Γ function can be generated as a function of y/B or $0.24\Delta R/R_o$. This approach is consistent with the approach taken for the load settlement curve method for shallow foundations. This was done for 5 piles including driven and bored piles as well as sand and clay soils. The piles are described in Briaud (1997) and in Briaud et al. (1985). They ranged from 0.3 to 1.2 m in diameter and from 6 to 36 m in length. In each case, the pile dimensions were known, the load displacement curve was

known and the PMT curves were measured at various depths within the depth D_v. An average PMT curve was created within D_v if more than one test was available. The Γ functions obtained from these load tests and parallel PMT tests are shown in Fig. 22. They have a shape similar to the one for the shallow foundations but the pile installation seems to make a difference. The driven piles lead to one class of Γ functions while the bored pile leads to a lower function. More data would help refine this first observation.

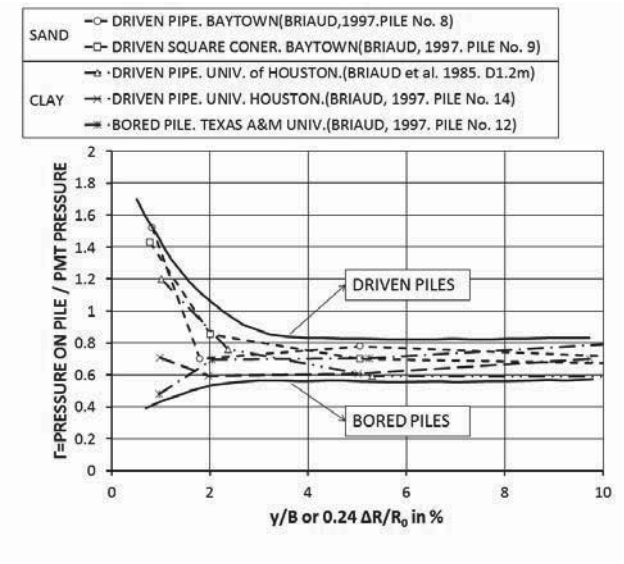

Figure 22. The Γ functions for transforming the PMT curve into a horizontal load – displacement curve for a pile.

10.2 Pile group behavior

The behavior of vertically loaded pile groups is often predicted by making use of an efficiency factor of the form

$$Q_g = e_v n Q_s \tag{53}$$

Where Q_g is the vertical load on the group, e_v the efficiency of the vertically loaded group, n the number of piles in the group, and Q_s the vertical load on the single pile for the same settlement as the pile group. This approach can be extended to the problem of horizontal loading on a pile group by writing

$$H_g = e_h n H_s \tag{54}$$

Where H_g is the horizontal load on the group, e_h the efficiency of the horizontally loaded group, n the number of piles in the group, and H_s the horizontal load on the single pile for the same horizontal movement as the pile group. Fig. 23 shows the plan view of a group of horizontally loaded piles.

A distinction is made between the leading piles on the front row of the group and the trailing piles behind the front row. Using data by Cox et al. (1983), Briaud (2013) proposed to extend Eq. 54 to read:

$$H_g = (n_{lp} e_{lp} + n_{tp} e_{tp}) H_s = \left(n_{lp} e_{lp} + n_{tp} \frac{e_{lp}}{\lambda} \right) H_s \tag{55}$$

Where n_{lp} and n_{tp} are the number of leading piles and trailing piles in the group respectively, e_{lp} and e_{tp} are the efficiency factors for the leading pile and trailing pile respectively, and λ is the ratio of e_{lp} over e_{tp}. Fig. 24 and 25 give the efficiency factors as a function of the relative pile spacing based on the data by Cox et al. (1983).

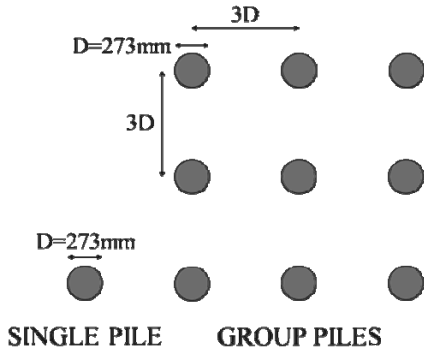

Figure 23. Plan view of a group of horizontally loaded piles.

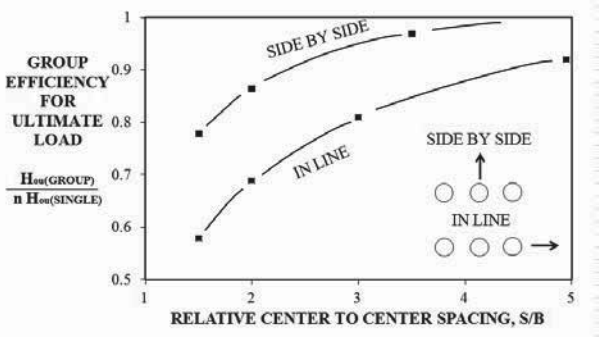

Figure 24. Leading pile and trailing pile efficiency factors

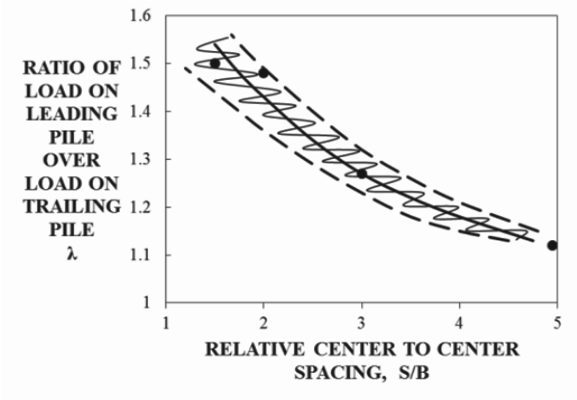

Figure 25. Ratio of leading over trailing pile efficiency factor

Eq. 52 was developed based on ultimate load observations at large horizontal displacements. The use of the same equation for all range of horizontal movements was investigated by comparing measured and predicted movements for two major pile group experiments by Brown and Reese (1985) in stiff clay and by Morrison and Reese (1986) in medium dense sand. The plan view of the group is shown in Fig.23. The piles were 0.273m in diameter, 13.1m long steel pipe piles driven in a 3 by 3 group with a spacing of 3 diameter center to center. The group was built to simulate a rigid cap condition which is most common. The clay was a stiff clay which had an undrained shear strength of about 100kPa within the top 3 m from the ground surface. The sand was a medium dense fine sand with a CPT point resistance increasing from zero at the ground surface to 3000 kPa at a depth of 2 m. Fig. 26 presents the result for the test in clay and Fig. 27 for the test in sand. In each case, the measured load-displacement curve for the single pile is presented as well as the measured curve linking the average load per pile in the group and the group displacement. The

efficiency in Eq. 55 was calculated as follows using Fig. 24 and 25:

$$H_g = \left(n_{lp} e_{lp} + n_{tp} \frac{e_{lp}}{\lambda} \right) H_s = \left(3 \times 0.95 + 6 \frac{0.95}{1.25} \right) H_s = 9 \times 0.82 \, H_s \quad (56)$$

The predicted curve describing the average horizontal load per pile in the group versus the group horizontal displacement was obtained by using the horizontal load versus horizontal displacement curve for the single pile and multiplying the single pile load by 0.82 for any given movement. The curve predicted using this approach is shown on Fig. 26 (clay) and 27 (sand) along with the measured curves.

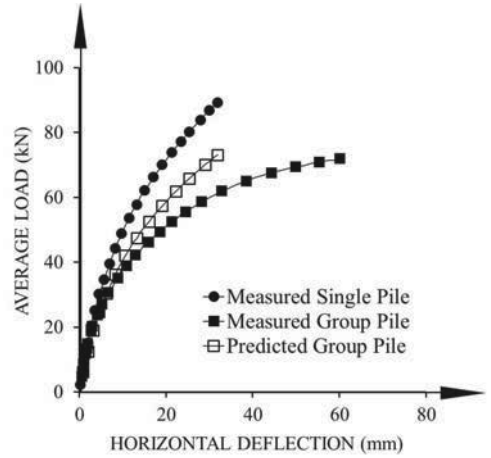

Figure 26. Predicted by Cox efficiency factor method and measured load-displacement curve for Brown-Reese group test in clay (1985)

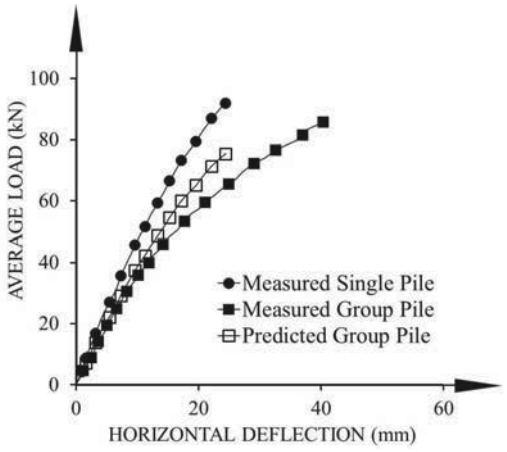

Figure 27. Predicted by Cox efficiency factor method and measured load-displacement curve for Morrison-Reese group test in sand (1986)

O'Neill (1983) suggested that the best and simplest efficiency factor to use for the settlement of a group of vertically loaded piles was:

$$\frac{s_g}{s_s} = \sqrt{\frac{B_g}{B_s}} \quad (57)$$

Where s_s is the settlement of the single pile under the working load Q, s_g the settlement of the group under nQ, n the number of piles in the group, B_g the width of the group and B_s the width of the single pile. This efficiency factor for the Brown and Reese pile group was (Fig. 23)

$$\frac{y_g}{y_s} = \sqrt{\frac{B_g}{B_s}} = \sqrt{\frac{1.91}{0.273}} = 2.65 \quad (58)$$

The curve linking the average load per pile in the group versus group displacement was obtained by using the load versus displacement curve for the single pile and, for any given horizontal movement, multiplying the single pile movement by 2.65. That predicted curve is shown on Fig. 28 and 29 along with the curve measured by Brown and Reese for their test in clay (1985) and Morrison and Reese for their test in sand (1986) respectively. The measured single pile curve is also shown for reference.

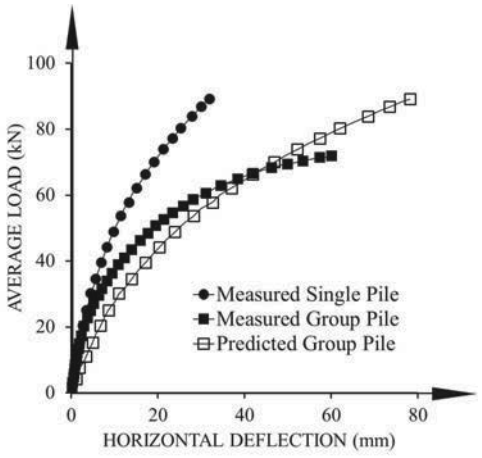

Figure 28. Predicted by O'Neill efficiency factor method and measured load-displacement curve for Brown-Reese group test in clay (1985)

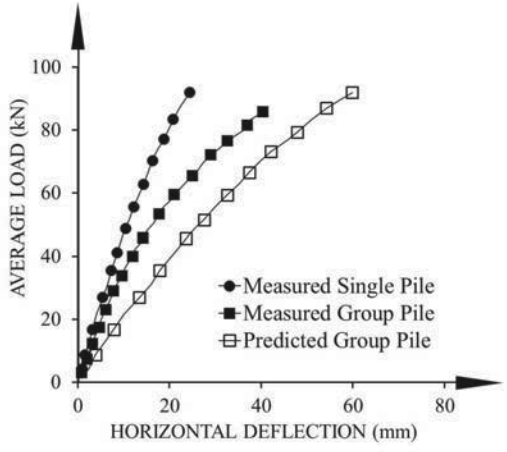

Figure 29. Predicted by O'Neill efficiency factor method and measured load-displacement curve for Morrison-Reese group test in sand (1986)

11 HORIZONTAL IMPACT LOADING FROM VEHICLE

In the case of road side safety, embassy defense against terrorist trucks, ship berthing, piles are impacted horizontally. To predict the behavior of piles subjected to horizontal impact, it is possible to use 4D programs (x, y, z, t) such as LSDYNA (2006). This is expensive and time consuming. The problem can be simplified by using a P-y curve approach generalized to include the effect of time. In this case the governing differential equation is

$$EI\frac{\partial^4 y}{\partial z^4} + M\frac{\partial^2 y}{\partial t^2} + C\frac{\partial y}{\partial t} + Ky = 0 \quad (59)$$

where E (N/m^2) is the modulus of elasticity of the pile, I (m^4) the moment of inertia of the pile against bending around the horizontal axis perpendicular to impact, y (m) the pile horizontal displacement at a depth z and a time t, M (kg/m) the mass per unit length of pile (mass of pile M_p plus mass of associated soil M_s), C ($N.s/m^2$) the damping of the system per unit length of pile, and K (N/m^2) the soil spring stiffness per unit length of pile. Note that the soil horizontal resistance is limited to p_u (kN/m^2). The boundary conditions are zero moment and zero shear at the point of impact, and zero moment and zero shear at the bottom of the pile. The initial condition is the displacement of the impact node during the first time step; this displacement is equal to v_o x Δt where v_o is the velocity of the vehicle and Δt the time step. Other inputs include the mass and velocity of the impacting vehicle, and the parameters in Eq. 59 for the soil and the pile. The differential equation is then solved by the finite difference method and it turns out that the parameter matrix is a diagonal matrix so that no inversion is necessary. As a result the solution can be provided in a simple Excel spread sheet (Mirdamadi, 2013).

Because the problem is a horizontal load problem on a pile, the PMT is favored to obtain the soil data. The PMT in this case is a mini PMT called the Pencel (Fig. 30) which is driven in place or driven in a predrilled slightly smaller diameter hole if the soil is hard. As a result of many static and impact horizontal load tests at various scales (Lim, 2011, Mirdamadi, 2013), the following recommendations are made for the input parameters.

$$M_s = 0.036B\frac{P_L}{g} \quad (60)$$

$$C\left(N.s/m^2\right) = 240\ P_L\left(kPa\right) \quad (61)$$

$$K = 2.3E_o \quad \text{and} \quad p_u = p_L \quad (62)$$

Where B is the pile width, p_L the PMT limit pressure, g the acceleration due to gravity, and E_o the first load PMT modulus.

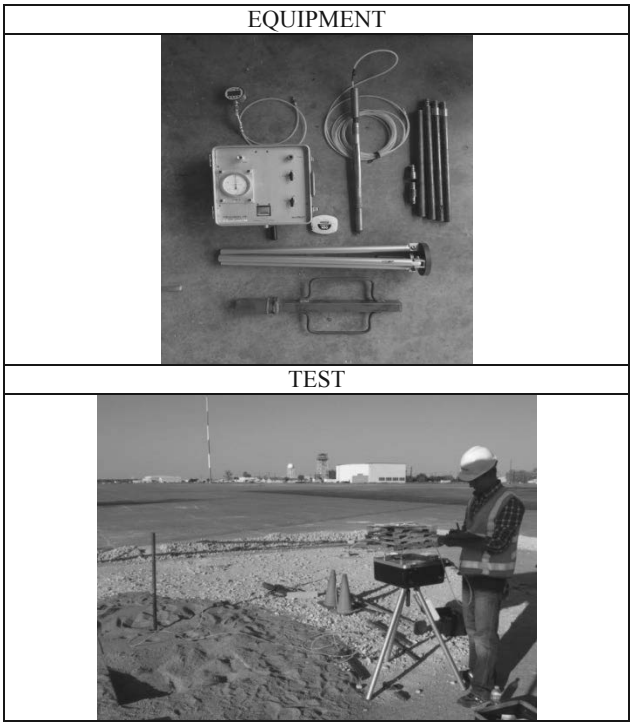

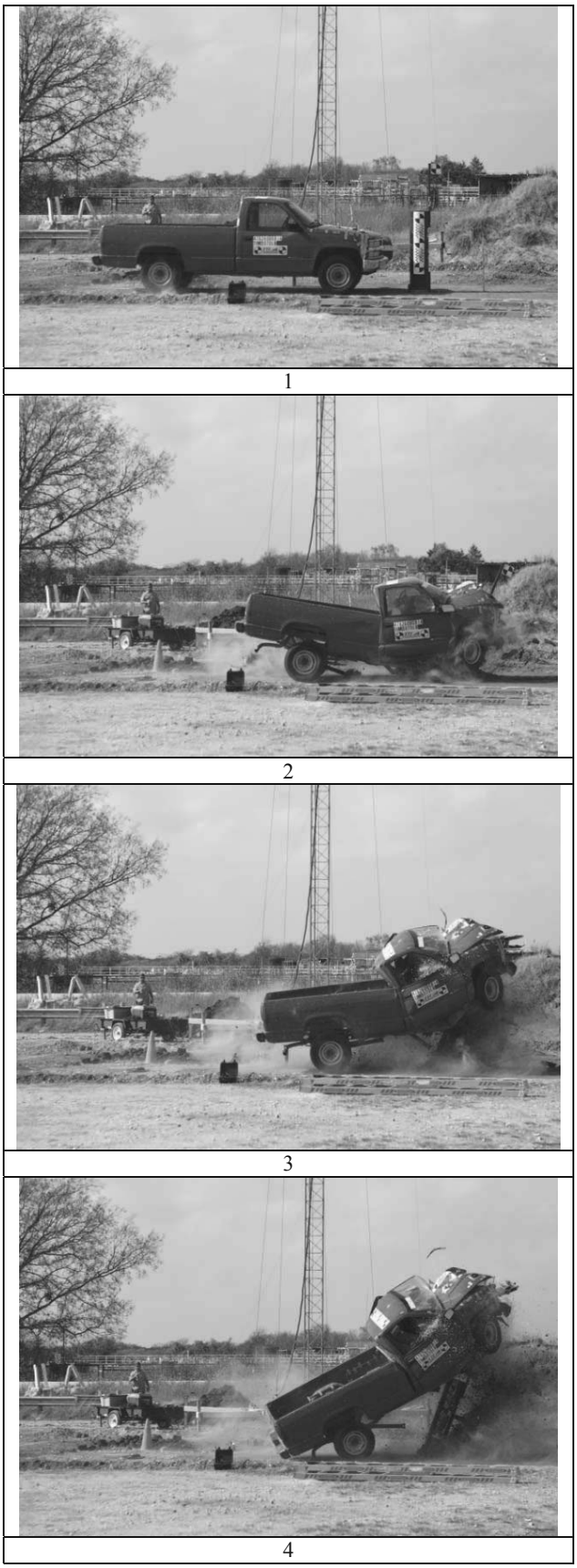

Figure 30. Mini pressuremeter test

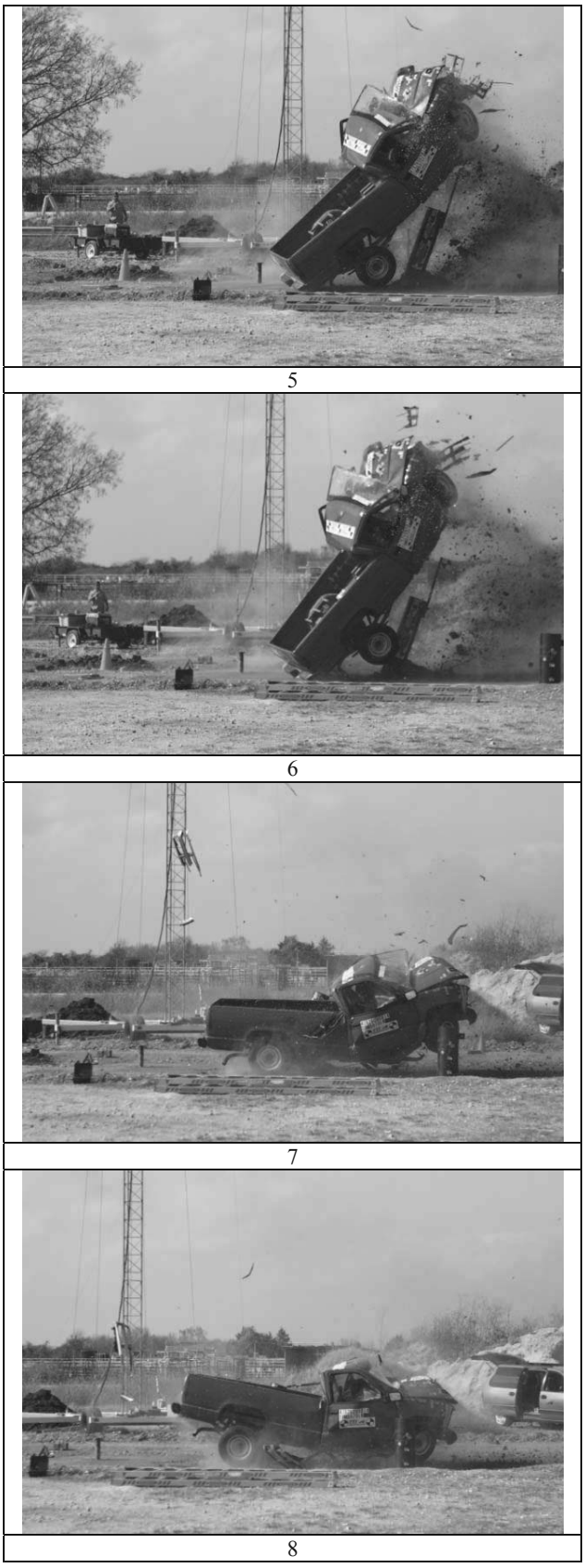

Figure 31. Pick-up truck impact test

Fig. 31 shows a photo sequence of an impact test where a 2300 kg pick up truck impacted a pile at 97.2 km/h. The pile was a steel pipe with a 356mm diameter and a 12.7mm wall thickness. It was embedded 2 m into a very stiff clay which gave the PMT parameters shown in Table 7. PMT tests were performed with a Pencel pressuremeter by first driving a slightly smaller diameter rod in the very stiff clay and then driving the Pencel probe in the slightly undersized hole. A comparison between the measured and calculated behavior of the pile (movement, load, and time) is presented in Fig. 32. The calculations were based on the simple Excel program (TAMU-POST, Mirdamadi, 2013) and a 4D FEM simulation using LS-DYNA (2006). The load was obtained by measuring the deceleration of the truck by placing an accelerometer on the bed of the truck and the movement by using high speed cameras.

Table 7. PMT results by driven Pencel pressuremeter

DEPTH OF TEST	MODULUS	LIMIT PRESSURE
1 m	45 MPa	1400 kPa
1.8 m	25 MPa	1200 kPa

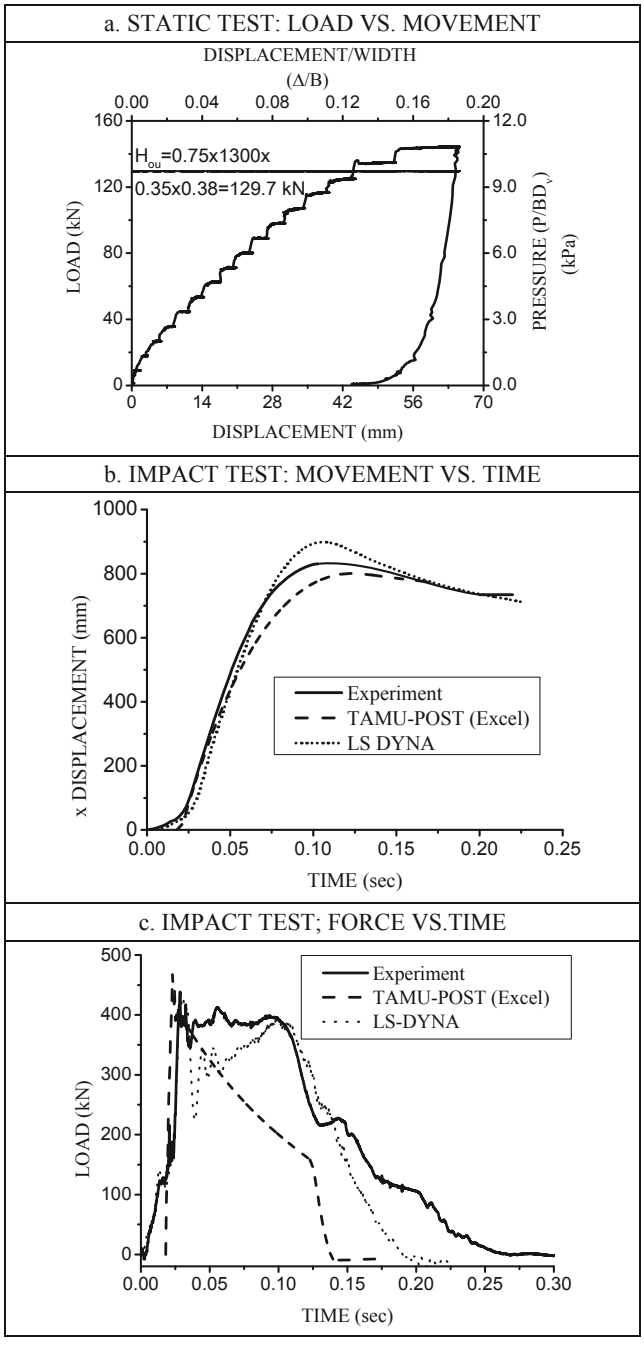

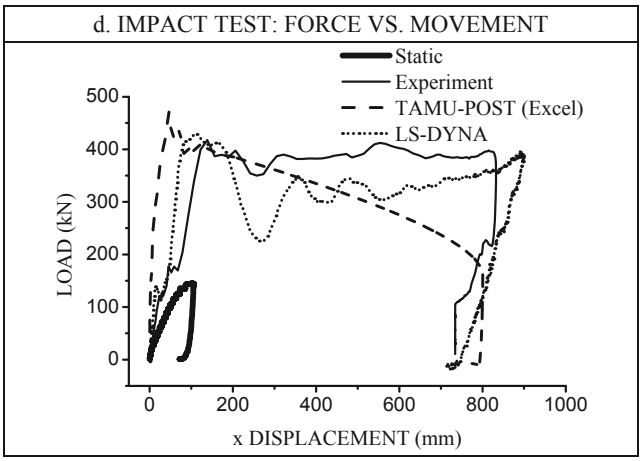

Figure 32. Pick-up truck impact test results

12 LIQUEFACTION CHARTS

Liquefaction charts have been proposed over the years to predict when coarse grained soils will liquefy. In those charts (Fig. 33), the vertical axis is the cyclic stress ratio CSR defined as τ_{av} / σ'_{ov} where τ_{av} is the average shear stress generated during the design earthquake and σ'_{ov} is the vertical effective stress at the depth investigated and at the time of the in situ soil test. On the horizontal axis of the charts is the in situ test parameter normalized and corrected for the effective stress level in the soil at the time of the test. There is a chart based on the normalized SPT blow count $N_{1\text{-}60}$ (Youd and Idriss, 1997). There is another chart based on the normalized CPT point resistance q_{c1} (Robertson and Wride, 1998). Using the correlations in Table 4, it is possible to transform the SPT and CPT axes into a normalized PMT limit pressure axis as shown in Fig. 34. The normalized limit pressure p_{L1} is

$$p_{L1} = p_L \left(\frac{p_a}{\sigma'_{ov}} \right)^{0.5} \quad (63)$$

Where p_L is the PMT limit pressure, p_a is the atmospheric pressure, and σ'_{ov} is the vertical effective stress at the depth of the PMT test. Note that the data points on the original charts are not shown on the PMT chart not to give the impression that measurements have been made to prove the correctness of the chart. Some degree of confidence can be derived from the fact that the two charts give reasonably close boundary lines. Nevertheless, these two charts are very preliminary in nature and must be verified by case histories.

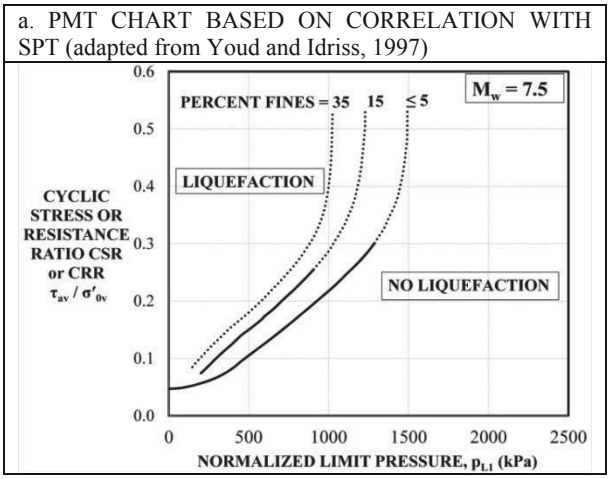

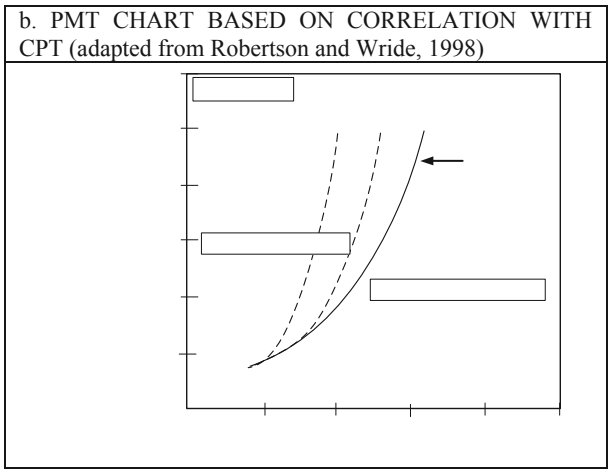

Figure 33. Preliminary liquefaction charts based on the pressuremeter limit pressure

13 ANALOGY BETWEEN PMT CURVE AND EARTH PRESSURE-DEFLECTION CURVE FOR RETAINING WALLS

The load settlement curve method for shallow foundations shows how one can use the PMT curve to predict the load settlement curve of a shallow foundation. This load settlement curve method was extended to the case of horizontally loaded piles. Can a similar idea be extended to the earth pressure versus deflection curve for retaining walls? One of the issues is that the PMT is a passive pressure type of loading so the potential for retaining walls may be stronger on the passive side than on the active side. Another issue is that the PMT test is a cylindrical expansion while the retaining wall is a plane strain problem. Fig. 34 shows the curves generated by Briaud and Kim (1998) based on several anchored wall case histories. The earth pressure coefficient K was obtained as the mean pressure p on the wall divided by the total vertical stress at the bottom of the wall. The mean pressure p was calculated by dividing the sum of the lock-off loads of the anchors by the tributary area of wall retained by the anchors. For each case history the lock off loads were known and the deflection of the wall was measured. Then the data was plotted with K on the vertical axis and the horizontal deflection at the top of the wall divided by the wall height on the horizontal axis. The shape of the curve is very similar to the shape of a PMT curve and a transformation function like the Γ function for the shallow foundation may exist but this work has not been done.

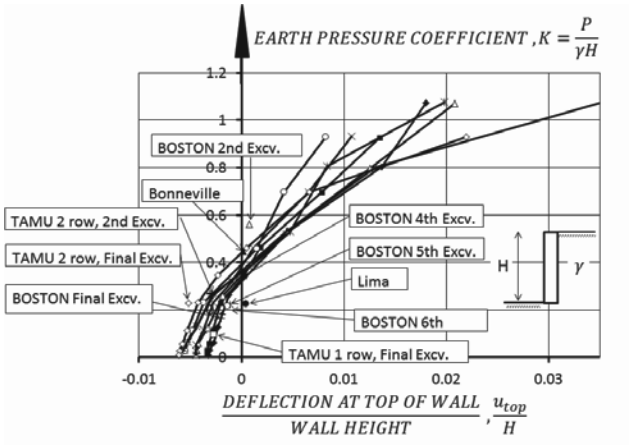

Figure 34. Earth pressure coefficient vs. wall deflection (after Briaud, Kim, 1998).

14 CONCLUSIONS

The purpose of this contribution was to show how the use of the PMT can be expanded further than current practice. In a first part, it is shown that more soil testing should take place in geotechnical engineering to reach a reasonable target of reliability. Then, it is theoretically demonstrated that if the lack of tensile resistance of soils is taken into account, the true soil modulus in compression is higher than what is obtained from conventional PMT data reduction. Then a procedure is investigated to recreate by hyperbolic extension the small strain early part of the curve lost by the decompression-recompression process associated with the preparation of the PMT borehole. The limitations of that procedure are identified. Best practice for preparing the PMT borehole, commonly expected values of PMT parameters, and correlations with other soil parameters are given. Reasoning is presented against the general use of the PMT unload reload modulus.

It is shown that instead of limiting the use of the PMT test results to the modulus and the limit pressure, the entire expansion curve can be used to predict the load settlement behavior of shallow foundations and the load displacement curve of deep foundations under horizontal loading. Long term creep loading and cyclic loading are addressed. A solution is presented for the design of piles subjected to dynamic vehicle impact. It is also shown how the PMT can be very useful for the foundation design of very tall structures. Finally an attempt is made to generate preliminary soil liquefaction curves base on the normalized PMT limit pressure.

15 ACKNOWLEDGEMENTS

The author wishes to thank the following individual for contributing to this paper: Roger Failmezger and Art Stephens for sharing some PMT data in sand, Ken Tand for sharing some plate load test data in stiff clay, Harry Poulos for providing some information on the Burj Khalifa measurements, Chris Haberfield for providing some information on the Nakheel Tower design, Clyde Baker for providing some information on his experience with the PMT and highrise foundation design. Several of my PhD students at Texas A&M University also contributed to this paper by making computations, preparing figures, formatting the manuscript, and more importantly discussing various aspects of the new contributions in this paper. They are: Alireza Mirdamadi, Ghassan Akrouch, Inwoo Jung, Seokhyung Lee.

16 REFERENCES

1. Baguelin F., Jezequel J.-F., Shields D.H., 1978, "The Pressuremeter and Foundation Engineering", Trans Tech Publications, Clausthal-Zellerfeld, W. Germany, 1978.
2. Baker C.N. Jr., 2010, "Uncertain Geotechnical Truth and Cost Effective High-Rise Foundation Design", 2009 Terzaghi Lecture, in Art of Foundation Engineering Practice, Edited by Mohamad H. Hussein; J. Brian Anderson; William M. Camp, Geotechnical Special Publications (GSP) 198, ASCE, Washington, USA.
3. Baker C.N., 2005, "The use of the Menard pressuremeter in innovative foundation design from Chicago to Kuala Lumpur", the 2nd Menard Lecture, Proceedings of the 5th Int. Symp. on the Pressuremeter – ISP5, Paris, France, Presses de l'ENPC.
4. Baud J.-P., Gambin M., Schlosser F., 2013, "Courbes hyperboliques contrainte–déformation au pressiomètre Ménard autoforé", Proceedings of the 18th International Conference on Soil Mechanics and Geotechnical Engineering, Paris 2013, Presses des Ponts et Chaussees, Paris, France.
5. Briaud J.-L., 1985, " Pressuremeter tests at Amoco refinery", consulting report to K.E. Tand and Associates, Houston, Texas.
6. Briaud J.-L., 1992, "The Pressuremeter", Taylor and Francis, London, pp.422.
7. Briaud J.-L., 1997, "SALLOP: Simple Approach for Lateral Loads on Piles", Journal of Geotechnical and Geoenvironmental Engineering, Vol. 123, No.10, ASCE, Washington, USA.
8. Briaud J.-L., 2007, "Spread Footings in Sand: Load Settlement Curve Approach", Journal of Geotechnical and Geoenvironmental Engineering, Vol 133, Issue 8, August 2007, ASCE, Reston, Virginia, USA.
9. Briaud J.-L., 2013, "Geotechnical Engineering: unsaturated and saturated soils", John Wiley and Sons, New York, pp.848.
10. Briaud J.-L., Gibbens R., 1999, "Behavior of Five Spread Footings in Sand," Journal of Geotechnical and Geoenvironmental Engineering, Vol. 125, No.9, pp. 787-797, September 1999, ASCE, Reston, Virginia.
11. Briaud J.-L., Kim N.K., 1998, "Beam Column Method for Tieback Walls", Journal of Geotechnical and Geoenvironmental Engineering, Vol. 124, No. 1, ASCE, Washington, DC.
12. Briaud J.-L., Makarim C.A., Little R., Tucker L., 1985, "Development of a pressuremeter method for predicting the behavior of single piles in clay subjected to cyclic lateral loading", Research Report RF5112 to Marathon Oil Company, McClelland Engineers, Raymond International Builders, Shell Development Company, Dpt of Civil Engineering, Texas A&M University, College Station, Texas, USA, pp214.
13. Brown D.A., Reese L.C., 1985, "Behavior of a large scale pile group subjected to cyclic lateral loading", Report to MMS, FHWA, and USAE-WES, Geotechnical Engineering Center Report GR85-12, Bureau of Engineering Research, Austin, Texas, USA.
14. Cox W.R., Dixon D.A., Murphy B.S., 1983, "Lateral load tests on 25.4 mm diameter piles in very soft clay in side by side and in line groups", ASTM Special Technical Publication no. STP 835, pp 122-140.
15. Duncan, J.M., and Chang, C.Y. (1970) "Non-linear analysis of stress and strain in soils," J. Soil Mech. Founds Div., ASCE, 96(SM5) 1629-1653.
16. Fascicule 62, 1993, "Regles techniques de conception et de calcul des foundations des ouvrages de genie civil", Ministere de l'equipement, du logement, et des transports, Publications Eyrolles, Paris, pp182.
17. Haberfield C.M., Paul D.R., 2010, "Footing design of the Nakheel Tower, Dubai, UAE", Proceedings of the Deep Foundation Conference, February 2010, Dubai, UAE, Deep Foundation Institute, 18pp.
18. Hossain, K. M. 1996. "Load settlement curve method for footings in sand at various depths, under eccentric or inclined loads, and near slopes." Ph.D. thesis, Texas A&M Univ., Dept. of Civil Engineering, College Station, Tx, USA.
19. Jeanjean, P. 1995. "Load settlement curve method for spread footings on sand from the pressuremeter test." Ph.D. dissertation, Texas A&M Univ., Dept. of Civil Engineering, College Station, Tx, USA.
20. Lim S.G., 2011, "Development of design guidelines for soil embedded post systems using wide flange I-beams to contain truck impact", PhD dissertation, Zachry Dpt. of Civil Engineering, Texas A&M University, College Station, Texas, USA, pp394.
21. Little R.L., Briaud J.-L., 1988, "Full scale cyclic lateral load tests on six piles in sand", Miscellaneous paper GL-88-27, US Army Engineer Waterways Experiment Station (now ERDC), Vicksburg, MS, USA, pp175.
22. LS-DYNA, 2006, "Theory Manual and User's Manual version 971", Livermore Software Technology Corporation, Livermore, CA.
23. Mayne, P. W., and G. J. Rix, 1993, "Gmax – qc Relationships for Clays," Geotechnical Testing Journal, ASTM, Vol. 16, No. 1, pp. 54-60.
24. Mirdamadi A., 2013, "Deterministic and probabilistic model of single pile under lateral impact", PhD dissertation, Zachry Dpt. of civil engineering, texas A&M university, College Station, Texas, USA.

25. Morrison C., Reese L.C., 1986, "A lateral load test of a full scale pile group in sand", Report to MMS, FHWA, and USAE-WES, Geotechnical Engineering Center Report GR85-12, Bureau of Engineering Research, Austin, Texas, USA.
26. NF P94-262, 2012, "Norme francaise, Justification des ouvrages geotechnicques, norme d'application nationale de l'Eurocode 7, foundations profondes, ISSN 0335-3931, AFNOR, pp206.
27. O'Neill M.W., 1983, " "Group action in offshore piles", ASCE Specialty Conference on Geotechnical Engineering in Offshore Engineering, Austin, Texas, USA.
28. O'Neill, M. W., Sheikh, S. A., 1985, "Geotechnical Behavior of Underreams in Pleistocene Clay," Drilled Piers and Caissons II, ed. by C. N. Baker, Jr., ASCE, May, pp 57 – 75.
29. Poeppel A. R., 2013, Personal Communication, April 2013, Langan Engineering.
30. Poulos H.G., 2009, Tall buildings and deep foundations – Middle East challenges", Terzaghi Oration, Proceedings of the 17th International Conference on Soil Mechanics and Geotechnical Engineering, Alexandria, Egypt, IOS Press publisher, 3173-3205 pp.
31. Rix, G.J. and Stokoe, K.H. (1991). Correlation of initial tangent modulus and cone resistance, Int Symp on Calibration Chamber Testing, Elsevier, New York, pp 351-362.
32. Robertson, P.K., and Wride, C.E., (1998), ―Evaluating Cyclic Liquefaction Potential using the Cone Penetration Test, Canadian Geotechnical Journal, Vol. 35, pp. 442-459.
33. Samtini N.C., Liu J.-L., 2005, "Use of in situ tests to design drilled shafts in dense and cemented soils", Proceedings of the Geo-Institute GeoFrontiers Conference, Austin, Texas, as part of the Mike O'Neill Memorial Volume, ASCE, Washington, DC, USA, 15pp.
34. Seed .B., Wong R.T., Idriss I.M., Tokimatsu K., 1986, "Moduli and damping factors for dynamic analyses of cohesionless soils, Journal of Geotechnical Engineering, ASCE, Vol. 112, GT11, pp1016-1032.
35. Tand K.E., 2013, "Plate load test results at Amoco refinery", Personal communication.
36. Youd, T.L. and Idriss, I.M., (1997). ―Proceedings of the NCEER Workshop on Evaluation of Liquefaction Resistance of Soils, Salt Lake City,UT, January 5-6, 1996, Technical Report NCEER-97-0022, National Center for Earthquake Engineering Research, University at Buffalo.